

CurvFed: Curvature-Aligned Federated Learning for Fairness without Demographics

HARSHIT SHARMA*, SHAILY ROY*, ASIF SALEKIN, Arizona State University, USA

Modern human-sensing applications often rely on data distributed across users and devices, where privacy concerns prevent centralized training. Federated Learning (FL) addresses this challenge by enabling collaborative model training without exposing raw data or attributes. However, achieving fairness in such settings remains difficult, as most human-sensing datasets lack demographic labels, and FL's privacy guarantees limit the use of sensitive attributes. This paper introduces **CurvFed**: Curvature-Aligned Federated Learning for Fairness without Demographics, a theoretically grounded framework that promotes fairness in FL without requiring any demographic or sensitive attribute information—a concept termed *Fairness without Demographics (FWD)*—by optimizing the underlying loss-landscape curvature. Building on the theory that equivalent loss-landscape curvature corresponds to consistent model efficacy across sensitive attribute groups, **CurvFed** regularizes the top eigenvalue of the Fisher Information Matrix (FIM) as an efficient proxy for loss-landscape curvature, both within and across clients. This alignment promotes uniform model behavior across diverse bias-inducing factors, offering an attribute-agnostic route to algorithmic fairness. **CurvFed** is especially suitable for real-world human-sensing FL scenarios involving single or multi-user edge devices with unknown or multiple bias factors. We validated **CurvFed** through theoretical and empirical justifications, as well as comprehensive evaluations using three real-world datasets and a deployment on a heterogeneous testbed of resource-constrained devices. Additionally, we conduct sensitivity analyses on local training data volume, client sampling, communication overhead, resource costs, and runtime performance to demonstrate its feasibility for practical FL edge device deployment.

ACM Reference Format:

Harshit Sharma*, Shaily Roy*, Asif Salekin. 2018. CurvFed: Curvature-Aligned Federated Learning for Fairness without Demographics. In *Proceedings of Make sure to enter the correct conference title from your rights confirmation email (Conference acronym 'XX)*. ACM, New York, NY, USA, 35 pages. <https://doi.org/XXXXXX.XXXXXXX>

1 Introduction

The integration of advanced machine learning (ML) with ubiquitous sensing [44, 64] has enabled everyday devices like smartphones and wearables to collect rich data for human-centric applications, from gesture recognition [94] to stress detection [74]. Concurrently, edge and distributed computing—especially federated learning (FL)—have emerged as key frameworks for decentralized model training [55, 96]. In FL, each client (e.g., device or organization) retains local data and trains models privately [46], reducing centralization risks [5, 7] and aligning with privacy regulations like GDPR, CCPA, and HIPAA [1, 89]. This makes FL ideal for human-sensing applications like health monitoring and activity recognition [22, 38, 68].

*Equal Contribution.

Author's Contact Information: Harshit Sharma*, Shaily Roy*, Asif Salekin, Arizona State University, Tempe, AZ, USA, {hsharm62, shailyro, asalekin}@asu.edu.

Permission to make digital or hard copies of all or part of this work for personal or classroom use is granted without fee provided that copies are not made or distributed for profit or commercial advantage and that copies bear this notice and the full citation on the first page. Copyrights for components of this work owned by others than the author(s) must be honored. Abstracting with credit is permitted. To copy otherwise, or republish, to post on servers or to redistribute to lists, requires prior specific permission and/or a fee. Request permissions from permissions@acm.org.

Conference acronym 'XX, Woodstock, NY

© 2018 Copyright held by the owner/author(s). Publication rights licensed to ACM.

ACM ISBN 978-1-4503-XXXX-X/2018/06

<https://doi.org/XXXXXX.XXXXXXX>

Notably, recent studies have begun exploring fairness in human-sensing federated learning (FL) [80, 84, 90]. However, state-of-the-art FL fairness approaches face a key challenge due to the trade-off between fairness and privacy [11], often requiring access to sensitive information at the client or server level, which contradicts *FL's privacy-preserving nature* [18, 23, 60, 88, 89]. This underscores the need for fairness-enhancing approaches that do not rely on sensitive or bias-inducing attributes. In human-sensing FL, this is especially important, as unlabeled factors can bias models —e.g., building materials can skew Wi-Fi CSI-based activity detection [42].

These challenges motivate the pursuit of Fairness without Demographics (FWD) [39] —refers to achieving equitable model performance across users or groups without relying on sensitive or demographic attributes such as sex, age, materials, among others, in FL, particularly since most human-sensing datasets lack labeled sensitive attributes [56, 84, 90]. *This also aligns with the 2025 Executive Order's [32] vision* for bias-resistant, innovation-driven AI by promoting fairness through optimization principles—without relying on demographic or group attributes—supporting equitable systems free from engineered social agendas. While FWD has been studied in centralized AI training [10, 30, 39], and only one FWD in FL work named FedSRCVaR [61] exists, FWD's integration into *privacy-preserving* decentralized FL remains challenging in human-centric FL, as outlined below:

- (1) Centralized FWD methods (Section 2.2) depend on access to global data distributions to identify biases and adjust decision boundaries, which is unavailable in *privacy-preserving* FL where clients only access local data [2], making fairness enforcement more difficult.
- (2) Although FedSRCVaR [61] does not require sensitive attribute labels in data, it relies on the knowledge of the bounds for sensitive or worst-case group sizes, making it not entirely agnostic to sensitive attribute knowledge (see Section 2.2).
- (3) Traditional group fairness methods—including FWD approaches (Section 2.2)—generally assume that all sensitive groups are represented during optimization [65]. However, this assumption is impractical in human-sensing FL, where each client often corresponds to a single user or a narrow demographic segment, resulting in an incomplete representation of population-level groups.
- (4) In human-centric sensing, multiple latent biases (e.g., gender, body type, sensor placement) coexist [35], and mitigating one bias may inadvertently worsen another [18].

In summary, a practical FWD solution for *privacy-preserving* human-sensing FL must operate without the knowledge of the sensitive attributes, tolerate missing group representations, and ensure fairness across both single- and multi- user clients and multiple bias sources. To address these challenges, this paper takes a fundamentally different approach than the literature—examining the *optimization loss-landscape geometry* of FL. It presents a theoretical justification (in Section 3) that reducing disparities in loss-landscape curvature both across and within clients offers an attribute-agnostic route to algorithmic fairness.

Building on this insight, it introduces *Curvature-Aligned Federated Learning (CurvFed)*, a novel FL method that achieves Fairness Without Demographics (FWD) by promoting *equitable and flatter* loss landscape curvatures across and within clients, without relying on sensitive attributes, bias factors, or global distribution knowledge, thus addressing the above-discussed first two and fourth challenges.

CurvFed utilizes the Fisher Information Matrix (FIM) as a fast-computable proxy for loss-landscape sharpness [41, 71], making it well-suited for resource-constrained edge devices (as FL clients), where it regularizes locally trained models to enhance fairness. Importantly, it introduces a sharpness-aware aggregation scheme, which aligns loss-landscape curvature across all clients by leveraging client-wise FIM data. This addresses the above-discussed third challenge, since FIM can be computed for both single-user and multi-user clients, allowing **CurvFed** to operate without requiring full representation of sensitive attributes within each client.

Recognizing the discussed challenges, our work introduces the first FWD for human-sensing FL, **CurvFed** that provides a *privacy-preserving*, robust alternative to traditional FL bias mitigation for human-sensing applications through the following contributions:

- *Theoretically Grounded Novel Approach:* **CurvFed**, being the first of its kind, provides a comprehensive theoretical justification establishing how having flatter curvature within the client through local training and equitable curvatures across clients through a novel sharpness-aware aggregation scheme promotes FWD (Section 3). Its theoretical claims are further supported by empirical validation (Section 6), making it a rigorous and novel solution.
- *Superior fairness-accuracy tradeoff:* Existing FL methods often struggle with the inherent tension between fairness and accuracy [23, 27]. **CurvFed** mitigates this by promoting flatter loss landscapes during client training, which inherently enhances generalizability [16, 34] and model inference confidence by pushing samples away from decision boundaries [73]. It further optimizes both curvature smoothness and accuracy during aggregation, yielding a better balance of fairness and performance (see Sections 4.1 and 5.2, RQ-1).
- *Equitable performance across diverse FL setups:* **CurvFed** handles varying client compositions from single-user to multi-user, without requiring full representation of sensitive groups, ensuring practical and equitable performance in real-world human-sensing FL (see Section 5.2, RQ-2, RQ-3).
- *Improved multi-attribute fairness simultaneously:* Human-sensing data involves multiple sensitive attributes [23, 89], but fair FL methods struggle to address them simultaneously [15, 89]. **CurvFed** promotes flatter client loss landscapes, improving fairness across all attributes without relying on attribute labels (see Section 5.2, RQ-4).
- *Real-world feasibility and sensitivity analysis:* We validate **CurvFed**’s practicality through extensive evaluations across data volume, client sampling, communication cost, resource usage, and runtime on diverse platforms. Additionally, a *real-world testbed evaluation* on a heterogeneous testbed of six edge devices confirms its effectiveness under non-simulated conditions (see Sections 5.3 and 5.4).

We demonstrate the effectiveness of **CurvFed** across *three* real-world human-sensing datasets, each representing different sensing modalities, applications, and sensitive attributes, showing **CurvFed**’s effectiveness in FWD. We adopt off-the-shelf models previously published for these datasets [12, 79, 94] for FL setting. However, **CurvFed** is architecture-agnostic. The framework is not tied to specific model choices and can be readily extended to diverse use cases and architectures. *The rest of the paper is organized as follows:* Section 2 reviews prior work; Section 3 presents the theoretical foundation and assumptions of **CurvFed**; Section 3.1 defines the problem, gaps, and challenges. Section 4 details the proposed method, Section 5 presents in-depth results, Section 6 presents empirical verifications of our propositions, and Section 7 discusses broader impacts and limitations.

2 Background and Related works

Fairness has emerged as a critical concern in machine learning (ML) research, with early efforts focusing on pre-processing strategies, such as removing sensitive attributes from training data [21]. However, such approaches often compromise model performance [89], prompting a shift toward in-processing methods that embed fairness constraints into model optimization [93]. While effective in centralized ML, these methods face new challenges in federated learning (FL), where privacy constraints limit access to sensitive attributes [18, 62]. This section discusses the recent fairness approaches in FL, highlights common evaluation metrics, and motivates the need for Fairness Without Demographics (FWD).

2.1 Fairness in Federated Learning

Bias in FL systems can arise in multiple ways [15, 18, 48, 88, 95], but a primary concern is **performance-based group fairness**, which aims to reduce disparities in model performance across demographic groups [9]. This is distinct from **contribution fairness**, which addresses disparities from client participation or data imbalance (e.g., non-IID data) [48, 95], and is beyond the scope of this work. In this study, we align with performance-based

group fairness approaches and focus on *ensuring that the global model does not disproportionately underperform for any groups*, a challenge exacerbated by the decentralized nature of data in FL.

Group fairness approaches in FL can be categorized by where the intervention occurs: at the client, at the server, or both.

Client-Side and Hybrid Approaches: Several methods enforce fairness during local training. For example, FedFB applies fair batch sampling on the client side [88], while others use min-max optimization to minimize worst-case group loss [20, 57, 60]. However, these approaches typically require access to sensitive attribute labels, making them unsuitable for Fairness Without Demographics (FWD). Notably, AFL [57] targets fairness across clients, rather than demographic groups, whereas others assume the availability of knowledge of sensitive group labels and distributions.

Recent works that implicitly flatten the loss landscape offer a closer fit to our setting, as they can promote fairness without accessing sensitive data. For example, [8] applies Sharpness-Aware Minimization (SAM) at the client and Stochastic Weight Averaging (SWA) at the server. These methods, which do not rely on demographic attributes, serve as relevant baselines for our evaluations. Our approach, ***CurvFed***, explicitly leverages sharpness cues and follows a hybrid framework leveraging sharpness information from the loss surface (a manner distinct from SAM) and adapting SWA in one of the modules. Our ablation study in Section 5.5 also demonstrates the impact of such adaptation in ***CurvFed***.

Server-Side Approaches: Some strategies address fairness during the server’s aggregation phase. FairFed [23] adjusts model aggregation weights based on local fairness evaluations performed by clients. Similarly, Astral [18] uses an evolutionary algorithm to select clients for aggregation to promote fairness. While these methods maintain data decentralization, they still require clients to compute fairness metrics using sensitive group information, creating potential privacy risks and conflicting with the goals of FWD.

2.2 Fairness Without Demographics (FWD)

The challenge of achieving fairness without access to sensitive attributes has motivated the field of Fairness Without Demographics (FWD). In centralized ML, this has been explored through techniques like adversarial re-weighting to boost the importance of underperforming instances [39]. However, in FL, each client operates with its own training instances, making it challenging to identify such instances and apply this approach directly. Another approach, knowledge distillation (KD), was used by [10] to transfer knowledge from a complex teacher to a student model to improve fairness without accessing sensitive information. We adapt this KD concept to FL as a baseline. After initial few rounds of initial training via the FedAvg [55] protocol, each client subsequently performs KD using the global model as the teacher, training a local student model on its own data with soft labels from the teacher before sharing their local model for aggregation.

To our knowledge, the only existing work applying FWD directly to FL is FedSRCVaR [61]. While both our work and FedSRCVaR target fairness without sensitive attributes, their problem formulations differ fundamentally. FedSRCVaR adopts a Rawlsian approach [39], optimizing for a worst-performing subset of individuals defined by a tunable threshold, ρ . Selecting an appropriate ρ is non-trivial in heterogeneous FL settings and requires prior knowledge or extensive tuning [28]. Furthermore, its evaluation assumes each client represents a single sensitive group. In contrast, our setting assumes clients may have mixed or sparse group representations. Despite a lack of public implementation details, we adapted FedSRCVaR to our setting and report it as a key baseline for a comprehensive evaluation. Our method, ***CurvFed***, differs by not imposing constraints on group size, offering a more flexible FWD approach.

2.3 Evaluation Metrics

We adopt established metrics to assess fairness and its trade-off with accuracy in FL [13, 17, 23, 45, 81].

Fairness: We use the **Equal Opportunity (EO) gap** [17, 23], defined as:

$$\Delta_{\text{EO}} = P(\hat{Y} = 1 | S = 1, Y = 1) - P(\hat{Y} = 1 | S = 0, Y = 1) \quad (1)$$

A lower Δ_{EO} indicates greater fairness. Sensitive attributes are used only during post-training evaluation.

Fairness–Accuracy Trade-off: To evaluate balance, we use the **FATE** score [13, 45, 81], which compares normalized changes in accuracy and fairness relative to a benign baseline:

$$\text{FATE} = \frac{\text{ACC}_m - \text{ACC}_b}{\text{ACC}_b} - \frac{\text{EO}_m - \text{EO}_b}{\text{EO}_b} \quad (2)$$

Here, m and b denote the fair model and the baseline (FedAvg [55]). A higher FATE score reflects a better fairness–accuracy trade-off.

3 Theoretical Justification of *CurvFed*

This section theoretically justifies and highlights *CurvFed*’s novelty starting from the problem setting, literature gaps, and challenges. Finally, it outlines the study assumptions.

3.1 Problem Context and Literature Gap

Fair FL Setting: In a human-sensing fair FL framework, a central server coordinates training across q distributed edge platforms, referred to as clients. Each client $t \in \{1, 2, \dots, q\}$ holds its own local dataset \mathcal{D}_t , which may contain data from *one or more individuals*. Each client private dataset, $\mathcal{D}_t = \{(x_k, y_k)\}_{k=1}^{n_t}$, where x_k is an input instance, y_k is the corresponding label, n_t is the number of data instances for the client t .

We can consider \mathcal{D}_t as a union of m disjoint groups, $\mathcal{D}_t = \bigcup_{i=1}^m G_i$, where each group G_i represents a subset of data distinguished by attributes such as, demographic characteristics (e.g., sex, age) or contextual factors (e.g., sensor placement or orientation). The goal of *performance-based group fairness in this fair FL framework* is to ensure that all such groups—regardless of which client they belong to—receive similar model performance.

Each client t trains a local model using \mathcal{D}_t with parameters θ_t^* by minimizing an empirical risk function over its dataset:

$$\begin{aligned} \theta_t^* &= \arg \min_{\theta} J(\theta, \mathcal{D}_t) \\ &= \arg \min_{\theta} \frac{1}{|\mathcal{D}_t|} \sum_i^{n_t} \ell(f_{\theta}(x_i), y_i) \end{aligned} \quad (3)$$

Here, f_{θ} is the predictive model parameterized by θ , and $\ell(\cdot)$ denotes a non-negative loss function that evaluates prediction error.

After local training, the server aggregates the client models $\{\theta_1^*, \dots, \theta_q^*\}$ into a global model with parameter θ^* . This aggregation is typically done through a weighted average, as shown in Eq. 4, where each client is assigned a non-negative weight β_t such that $\sum_{t=1}^q \beta_t = 1$, with the goal of minimizing its *excessive loss* [61], shown in Eq. 5.

$$\theta^* = \sum_{t=1}^q \beta_t \theta_t^* \quad (4)$$

$$R(t) := J(\theta^*, \mathcal{D}_t) - J(\theta_t^*, \mathcal{D}_t) \quad (5)$$

A key fairness concern is that the global model may disproportionately favor some clients. To address this, prior work [61] introduces the concept of excessive loss in Eq. 5—the performance gap between a client’s local and the global model—and promotes fairness by minimizing its variance across clients:

$$\arg \min \text{Var}_t[R(t)] = \frac{1}{q} \sum_{t=1}^q (R(t) - \bar{R})^2, \quad \text{where} \quad \bar{R} = \frac{1}{q} \sum_{t=1}^q R(t) \quad (6)$$

This objective ensures that model utility is distributed equitably across clients. In this work, we utilize $\|\cdot\|$ notation to denote the Euclidean norm, vectors or matrices by bold symbols, and sets by uppercase symbols.

Challenge of this paper's FWD problem setting: Our FWD objective is to promote fairness in FL beyond the scope discussed above. We aim to minimize disparities in model performance across all groups of individuals—regardless of which client they belong to—even when sensitive attributes (e.g., sex, age) that constitute the groups or underlie the disparities are unknown, latent, or unavailable. This consideration is especially critical in human-sensing applications, where a single client may represent data from one or more individuals with diverse and often unobservable characteristics. Consequently, achieving uniform performance across clients does not guarantee equitable treatment for all underlying groups or individuals. Our proposed solution builds on Eq. 6 to attain this FWD objective.

3.2 FWD in FL: A Curvature-Based Roadmap

We begin by establishing an upper bound on a client's excessive loss Eq. 5, which helps isolate the disparity factors in terms of loss curvature within the client's data, \mathcal{D}_t , and between the client's and the global model. The following theorem and justifications assume that the loss function $\ell(\cdot)$ is at least twice differentiable, as is common for standard objectives such as cross-entropy and mean squared error.

Theorem 1 Through Taylor expansion, the upper bound of excessive loss $R(t)$ of the global model with parameters θ^* computed using client t 's private dataset, \mathcal{D}_t is formalized as:

$$R(t) \leq \|g_t^\ell\| \times \|\theta^* - \theta_t^*\| + \frac{1}{2} \lambda(\mathbf{H}_t^\ell) \times \|\theta^* - \theta_t^*\|^2 + O(\|\theta^* - \theta_t^*\|^3). \quad (7)$$

Here, $g_t^\ell = \nabla_\theta \ell(\theta_t^*, \mathcal{D}_t)$ is the local models gradient vector, and $\mathbf{H}_t^\ell = \nabla_\theta^2 \ell(\theta_t^*, \mathcal{D}_t)$ is the local model's Hessian at optimal parameter θ_t^* associated with the loss function ℓ . The term $\lambda(\cdot)$ denotes the maximum eigenvalue (hereby referenced as the top eigenvalue). Equation 7 reveals that the excessive loss is tightly linked to the client t 's (i) gradient vector corresponding to the loss, i.e., g_t^ℓ and (ii) the top Hessian eigenvalue, a proxy of the curvature (sharpness) of the local loss landscape.

Sharpness, Curvature, and Fairness: High curvature in the loss landscape of model optimization, characterized by sharp minima, typically associated with large top Hessian eigenvalues—is known to impair generalization [16, 34]. Importantly, disparities in two groups (based on demography or other factors) in terms of their top Hessian eigenvalues have been shown to correlate with the model's performance disparities between those groups [73], suggesting that mitigating disparities among all groups' curvatures (top Hessian eigenvalues) will promote fairness.

However, *there are several challenges to implementing this:*

- (1) Computing the full Hessian matrix is computationally costly [19], thus, infeasible on resource-constrained edge devices.
- (2) For us, the groups are unknown, because we are unaware of the factors (sensitive attributes) creating disparities.
- (3) In our setting, some clients can be just one person, implying all data can belong to just one group (at least in terms of demography or individual attributes like left or right-handed).

To address these challenges, we developed **CurvFed** – a principled framework that achieves fairness without explicit sensitive attribute labels (or knowledge) by regulating sharpness at both local client-level and global levels during model aggregation. Our method is guided by the following three propositions:

Proposition 1. Fisher Approximates Hessian

To address the *first challenge*, we leverage the empirical Fisher Information Matrix (FIM) as an efficient proxy for the Hessian:

$$\mathbf{H} \approx \mathbf{F} = \frac{1}{n_t} \sum_{i=1}^{n_t} \nabla_{\theta} \ell(f_{\theta}(x_i), y_i) \nabla_{\theta} \ell(f_{\theta}(x_i), y_i)^T. \quad (8)$$

Lee et. al. [41] describe the relationship between the empirical FIM (\mathbf{F}) and the Hessian matrix (\mathbf{H}) as shown in equation 8. Where $\nabla_{\theta} \ell(f_{\theta}(x_i), y_i)$ is the gradient vector corresponding to the loss of the i^{th} data sample, for a model f with parameters θ and the total number of data samples represented by n_t . The empirical FIM thus serves as a *computationally efficient* approximation of the Hessian, reducing computational costs during training [41, 70].

Proposition 2. Minimizing the FIM Top Eigenvalue Reduces Group-wise Curvature Disparity.

Building on Proposition 1, which establishes the FIM as a tractable approximation of the Hessian, we now provide a theoretical argument that minimizing the top eigenvalue of the FIM (denoted as $\lambda(F_t)$) during client-level training reduces curvature disparity across all constituent groups G_1, G_2, \dots, G_m within the local dataset $\mathcal{D}_t = \bigcup_{i=1}^m G_i$.

The full-dataset FIM can be expressed as a convex combination of group FIMs:

$$F_t = \sum_{i=1}^m \alpha_i F_{G_i}, \quad \text{where } \alpha_i = \frac{|G_i|}{|\mathcal{D}_t|}, \quad \sum_i \alpha_i = 1. \quad (9)$$

Using Jensen's and Weyl's inequalities [6, 31], with an assumption of approximate dominant eigenvector alignment for the lower bound, we establish bounds:

$$\max_i \lambda(F_{G_i}) - \delta \leq \lambda(F_t) \leq \sum_{i=1}^m \alpha_i \lambda(F_{G_i}) \quad (10)$$

where $\delta \geq 0$ accounts for potential eigenvector misalignment.

Our key insight is that during client training, penalizing $\lambda(F_t)$ implicitly drives the groups' top eigenvalues $\lambda(F_{G_i})$ towards uniformity. Notably, as shown in Eq. 10, minimizing $\lambda(F_t)$ effectively reduces the top eigenvalue of the group with the highest curvature, i.e., highest top eigenvalue of FIM ($\max_i \lambda(F_{G_i}) - \delta$). Intuitively, in the loss landscape, continuing to lower the dominant curvature reduces the variance across all groups' curvatures, promoting uniformity. *This approach is group-agnostic, relying purely on optimization geometry, thus addressing the second challenge discussed above.* Notably, empirical evidence supporting this theoretical reduction in curvature disparity is presented in Section 6.

Proposition 3. Sharpness-Aware Aggregation Reduces Variance in Excessive Loss Across Clients.

Building upon the understanding of excessive loss $R(t)$ from Theorem 1 and the local curvature control from Proposition 2, we now posit that our sharpness-aware aggregation scheme directly contributes to reducing the variance of excessive loss, $\text{Var}_t[R(t)]$, across clients-both in terms of performance and curvature. This promotes fairer performance distribution.

From Theorem 1 and Proposition 2, and assuming that the discrepancy $\delta_t = \|\theta^* - \theta_t^*\|$ remains sufficiently small- since the local training across clients occurs for a few epochs before each aggregation (allowing us to neglect higher-order terms and its variances), the excessive loss for client t is approximately:

$$R(t) \leq \|g_t^\ell\| \cdot \delta_t + \frac{1}{2} \lambda(F_t^\ell) \cdot \delta_t^2$$

Here, g_t^ℓ is the local model's gradient at its optimum θ_t^* , and $\lambda(F_t^\ell)$ is the top eigenvalue of its FIM, serving as a proxy for Hessian's top eigenvalue (following Proposition 1). This indicates that for a client t , its excessive loss is

impacted mostly by g_t^ℓ and $\lambda(\mathbf{F}_t^\ell)$, which may vary significantly across clients. Our variance reduction strategy builds on this observation. During its local training, each client t seeks to minimize its empirical risk $J(\theta, \mathcal{D}_t)$. Successful training results in a small local gradient norm $\|g_t^\ell\|$ at θ_t^* . Furthermore, as established in Proposition 2, our framework encourages clients to find solutions θ_t^* that also exhibit low curvature, i.e., a minimized $\lambda(\mathbf{F}_t^\ell)$. That means an effective locally trained client will have lower g_t^ℓ and $\lambda(\mathbf{F}_t^\ell)$, thus lower excessive loss, and the opposite holds for ineffective locally trained ones.

CurvFed’s Sharpness-Aware Aggregation builds on standard fair FL aggregation (Eq. 4-6) with the novel incorporation of curvature information into the weighting scheme. Specifically, client weights β_t in Eq. 4 are computed based on excessive loss $R(t)$, which accounts for both the local loss (corresponding to g_t) and top FIM eigenvalue $\lambda(F_t)$ (detailed in Section 4.1.2). Clients with lower $R(t)$, i.e., lower g_t and $\lambda(F_t)$ receive higher weights. This serves two goals: First, it *prioritizes effectively trained clients*—those with low loss (indicated by small g_t) and low curvature $\lambda(F_t^\ell)$, indicating locally fairer. These clients contribute more to the global model, resulting in lower and more uniform excessive loss $R(t)$ across them. And Second, the scheme effectively *mitigates “outlier” influence*: conversely, clients that exhibit high $R(t)$, which would lead to a higher $\text{Var}_t[R(t)]$, are assigned lower weights, curtailing their ability to inflate the $\text{Var}_t[R(t)]$ in Eq. 6.

Because the aggregation is driven by excessive loss, *CurvFed* is *agnostic to demographic (i.e., sensitive attributes) knowledge and the number of individuals belonging to clients, addressing challenges 2 and 3 discussed above*. In summary, by emphasizing well-trained, low-curvature clients, CurvFed reduces $\text{Var}_t[R(t)]$ in Eq. 6, guiding the global model toward fairer convergence, promoting group fairness without explicit demographic (i.e., sensitive attributes) knowledge.

3.3 Assumptions

This study operates under the following assumptions:

- (1) We consider a centralized FL setup where a server coordinates training without access to clients’ local datasets \mathcal{D}_t . No external public datasets are assumed to approximate the overall data distribution.
- (2) Our goal is to promote **performance-based group fairness** by ensuring the global model performs equitably across groups defined by sensitive attributes (e.g., sex, age, sensor location). For a sensitive attribute a , let $G_c^a = \{(x_i, y_i) \mid x_i \text{ belongs to the category } c\}$ with $c \in \{1, \dots, C_a\}$ -categories of a . Fairness entails minimizing performance disparities across these groups, such as ensuring similar accuracy for $G_{\text{male}}^{\text{sex}}$ and $G_{\text{female}}^{\text{sex}}$.
- (3) We assume the central server is not resource-constrained and, consistent with standard FL approaches (e.g., FedAvg[55]), can perform model aggregation efficiently.

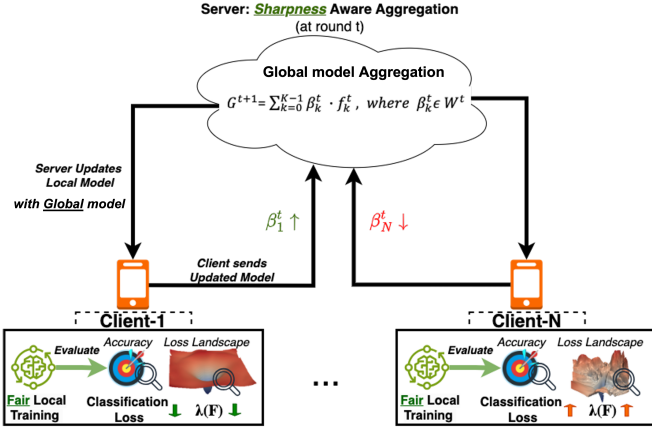
4 CurvFed: Design Choices and Approach

Fig. 1 provides an overview of **CurvFed**. In each FL round, clients use their own individuals’ data to train local models, aiming to optimize accuracy and promote local fairness. The server then aggregates these models using our *Sharpness-aware aggregation* strategy to enhance fairness and accuracy. The global model is redistributed to clients for the next round. Details of **CurvFed** is below.

4.1 Design Choices

Our FWD attaining design choices leverage loss-landscape curvature at both client and global aggregation levels, grounded in the theoretical justifications in Section 3, are presented below:

4.1.1 Fair Local Training Objective: In the FL context, each client learns a model, denoted as f_{client} . We have two objectives on the client side: (1) maximizing accuracy and (2) promoting fairness, i.e., mitigating bias within the client’s own data distribution.

Fig. 1. *CurvFed* overview.

We introduce a curvature regularization term in the client's loss function to enhance group fairness. The learning objective at the client-level is formulated as:

$$\begin{aligned} \arg \min \text{ Loss}_{\text{client}} = & \alpha \cdot \ell_{\text{client}}(f_{\text{client}}(x_i)) \\ & + (1 - \alpha) \cdot \frac{1}{N_{\text{correct}}} \cdot \lambda(F_{\text{client}})_{\text{correct}} \end{aligned} \quad (11)$$

Here, N_{correct} represents the number of correctly classified instances in a batch, and x_i is the input in the i^{th} batch. The term $\ell_{\text{client}}(f_{\text{client}}(x_i))$ ensures accuracy maximization by minimizing classification loss. The regularization term penalizes the top eigenvalue of the FIM, i.e., $\lambda(F_{\text{client}})_{\text{correct}}$, associated with the loss for correctly classified samples, promoting group fairness as outlined in *Proposition 2* in Section 3.

In equation 11, we introduce α , a hyperparameter that acts as a balancing factor between the two objectives. α is identified using a grid search in this work. However, popular hyperparameter optimization frameworks like Optuna [3] can be used to find the optimal α . In our evaluations, a single α identified via grid search was effective across all three datasets. This consistency suggests that the local optimization strategy transfers reasonably well across heterogeneous human-sensing datasets. We will use $\lambda(F_{\text{client}})$ instead of $\lambda(F_{\text{client}})_{\text{correct}}$ for simplicity for the rest of the section.

4.1.2 Sharpness-aware Aggregation to Promote Fairness: After local training, each client has a distinct accuracy and top eigenvalue of FIM ($\lambda(F_{\text{client}})$), as depicted in Fig. 1, leading to varying excessive losses. As outlined in *Proposition 3* in Section 3, clients with lower excessive losses should contribute more to deriving the aggregated global model.

This aggregation strategy draws inspiration from Pessimistic Weighted Aggregation (P-W) in FL [17], which excludes clients with known biases during aggregation. However, in the FWD setting, such bias information is unavailable. Instead, our *Sharpness-aware Aggregation* implicitly promotes fairness by assigning higher weights to clients with lower excessive loss, i.e., having lower top eigenvalue of FIM and lower classification error (according to *Proposition 3*), thus supporting fairer and more performant global updates without relying on explicit sensitive attributes.

To compute the aggregation weights for N clients: $W^r = \{\beta_n^r \mid \forall n \in \{1, \dots, N\}\}$ at each round r , the server collects each client's evaluation loss $\text{loss}_n^{\text{eval}}$ and the top FIM eigenvalue $\lambda(F_n^{\text{eval}})$. These are then used to compute the aggregation weights as described in Equation 12.

$$W^r = S(S(L) \cdot S(T)) \quad (12)$$

Here, we use the *Softmax operator* denoted as S for simplicity. Notably, $L = \left\{ \epsilon + \frac{1}{\text{loss}_n^{\text{eval}}} \right\}_{n=1}^N$ and $T = \left\{ \epsilon + \frac{1}{\lambda(F_n^{\text{eval}})} \right\}_{n=1}^N$ and ϵ is a small constant to avoid division by zero in weight calculations.

4.2 Approach

Algorithm 1 outlines **CurvFed** approach, which begins with the following inputs: a randomly initialized global model denoted as G^0 , the number of clients participating in FL process represented by N , the total number of rounds for the FL process indicated by R , the number of epochs E for conducting local training on each client's side, the cycle length c for implementing the stochastic weight averaging (SWA) protocol [8], the weighting factor α used to balance the client loss, the batch size B utilized by the clients during training, client learning rate γ and learning rate scheduler $\gamma()$. Different modules of **CurvFed** are detailed below:

Algorithm 1 Curvature-Aligned Federated Learning (**CurvFed**)

```

1: Input: ◊  $G^0$ : Initial random model, ◊  $N$ : Number of Clients, ◊  $R$ : Total rounds, ◊  $E$ : local training epochs, ◊  $c$ : cycle length, ◊  $\eta$ : SWA starting threshold, ◊  $\alpha$ : client loss weighting factor, ◊  $B$ : Client batch size, ◊  $\gamma$ : Learning rate, ◊  $\gamma()$ : Learning rate scheduler
2: Parameter: ◊  $L[]$ : Array to store classification loss of clients, ◊  $T[]$ : Array to store top eigenvalue of FIM of clients, ◊  $S$ : Softmax operator
3: Returns:  $G_{\text{SWA}}$ : Global model
4: for each round  $r=0$  to  $R-1$  do
5:   if  $r = \eta \times R$  then
6:      $G_{\text{SWA}} \leftarrow G^r$ 
7:   end if
8:   if  $n \geq \eta \times R$  then
9:      $\gamma = \gamma(r)$ 
10:   end if
11:   for each  $Client_n$   $n=0$  to  $N-1$  do
12:      $params \leftarrow G^r, Client_n, E, B, \alpha, \gamma$ 
13:      $f_n^r, loss_n^r, \lambda(F_n^r) \leftarrow TrainClient(params)$ 
14:      $L[n] \leftarrow \epsilon + \frac{1}{loss_n^r}$ 
15:      $T[k] \leftarrow \epsilon + \frac{1}{\lambda(F_n^r)}$ 
16:   end for
17:    $W^r = S(S(L) \cdot S(T))$ 
18:    $G^{r+1} = \sum_{n=1}^N \beta_n^r \cdot f_n^r \quad \forall \beta_n^r \in W^r$ 
19:   if  $r \geq \eta \times R$  and  $mod(r, c) = 0$  then
20:      $n_{\text{models}} \leftarrow n/c$ 
21:      $G_{\text{SWA}} \leftarrow \frac{n_{\text{model}} \times G_{\text{SWA}} + G^r}{n_{\text{models}} + 1}$ 
22:   end if
23: end for
24: return  $G_{\text{SWA}}$ 

```

4.2.1 Local Client Training: Following standard FL protocol [55], the server initializes by distributing a randomly initialized global model G^0 and other training parameters to the clients for local training through the *TrainClient* module (line 12-13).

TrainClient Module, as shown in Algorithm 2, receives the global model, along with training configurations such as the number of local training epochs E , batch size B , learning rate γ , and the client loss weighting factor α from the server. On the client side, data is divided into a training set \mathcal{D}_{train} and an evaluation set \mathcal{D}_{eval} . The model is trained on \mathcal{D}_{train} (line-9), where we utilized the Sharpness-Aware Minimization (SAM) optimizer for model training[25]. The choice of the model optimizer is influenced by prior works in FL, which claim that using SAM optimizer at the client level helps with convergence and promotes local flatness [8], thus lowering curvature and further promoting fairness.

Algorithm 2 *TrainClient*($G^t, Client_k, E, B, \alpha, \gamma$)

```

1: Parameter: ◊  $G^t$ : Initial model sent from Server side, ◊  $E$ : local training epochs at Client side, ◊  $Client_k$ : Client-ID, ◊  $B$ : Client Batch size, ◊  $\alpha$ : client loss weighting factor, ◊  $\gamma$ : client learning rate
2: Returns:  $f_n^r, Loss_{eval,n}^r, \lambda(F_{eval,n}^r)$ 
3: Initialize:  $f_n^r \leftarrow G^t$  {Server-side global model}
4: Initialize:  $l_n$  {Client Classification loss}
5: Initialize: SAM optimizer
6: Split:  $Client_n$  data  $\mathcal{D}_n$  into  $\mathcal{D}_{train}$  and  $\mathcal{D}_{eval}$ 
7: for each epoch  $e=0$  to  $E-1$  do
8:   for each batch  $i=0$  to  $B$  in  $\mathcal{D}_{train}$  do
9:      $argminLoss_n$ 
10:    end for
11:    Evaluate  $f_n$  on  $\mathcal{D}_{eval}$  get:  $eval\_loss_n, eval\_lambda(F_n)$ 
12:     $Loss_{eval,n}^r \leftarrow eval\_loss_n$ 
13:     $\lambda(F_{eval,n}^r) \leftarrow eval\_lambda(F_n)$ 
14:  end for
15: return  $f_n^r, Loss_{eval,n}^r, \lambda(F_{eval,n}^r)$ 

```

The client-local training follows the dual objective discussed in Section 4.1.1, as per Equation 11. The model performance is assessed on the disjoint \mathcal{D}_{eval} (line-11) to identify the best-performing model. For this model, the evaluation loss $eval_loss_n$ and the top eigenvalue of the FIM $eval_lambda(F_n)$ are calculated. The optimal model's evaluation loss and FIM top eigenvalue are stored in $Loss_{eval,n}^r$ and $\lambda(F_{eval,n}^r)$, respectively (Lines 12,13). These metrics and the weights of the selected model are then sent back to the server (line-15).

4.2.2 Sharpness-aware Aggregation: Upon receipt of the clients' local training returns, as per Algorithm 1, the server starts the model aggregation phase. Our *Sharpness-aware aggregation* method calculates weights for each client based on their classification loss and the top eigenvalue of the FIM related to their loss (lines 14,15). Clients with lower classification loss and lower top eigenvalue of FIM are assigned higher weights (line 17).

Stochastic Weight Averaging (SWA): On the server side, we also use SWA [33], a technique shown to enhance generalization in FL systems [8]. The significance of generalization in fair models is underscored by research [14, 24] focusing on improving their robustness and ability to perform fairly across unseen data. This addresses the challenge of fairness constraint overfitting [14], where models fair on training data may still exhibit unfairness on unseen data. In human-sensing FL, ensuring fairness and robustness across unseen instances is critical; hence, the adoption of SWA is crucial in **CurvFed**. SWA averages the global models at regular intervals, i.e., cycles c (line 19), and adjusts the learning rate throughout the FL process (line 9) to achieve flatter minima, thereby preventing overfitting as the process advances. The SWA process begins after a threshold (η) number of

rounds are complete (lines 4-7); for our evaluations, this threshold is set to $\eta = 20\%$. The early start threshold was chosen due to the limited data size, which allows for quicker convergence in our setting.

5 Experimental Evaluation

This section provides a comprehensive evaluation of ***CurvFed***, covering datasets and models (Section 5.1), followed by an analysis addressing four key research questions on CurvFed’s effectiveness (Section 5.2). We then assess its real-world deployment feasibility and sensitivity (Sections 5.3 and 5.4) and conclude with an ablation study justifying the design choices (Section 5.5).

5.1 Datasets and Models

Few human-sensing datasets capture diverse bias-inducing factors such as sex and sensor placement [84]. We evaluate ***CurvFed*** on three such datasets: Stress Sensing [79] (48 participants), WIDAR [94] (16 participants), and HugaDB [12] (18 participants). Each includes known sources of bias—WIDAR: sex and sensor orientation; Stress Sensing: sex and watch hand; HugaDB: sex.

Dataset Rationale: We selected these datasets to evaluate the effectiveness of ***CurvFed*** across diverse human-sensing applications:

Human Activity Recognition (HAR): WIDAR and HugaDB utilize different sensing modalities— WiFi-based body-coordinate velocity profiles [94] in WIDAR and inertial data (accelerometer and gyroscope) in HugaDB—for gesture and activity recognition, respectively.

Stress Sensing: The Stress sensing dataset includes *multi-modal input data*, specifically electrodermal activity (EDA) and accelerometer readings from an Empatica E4 watch for stress detection.

This selection ensures a comprehensive evaluation of ***CurvFed*** across different modalities and application domains.

Model Architectures: We use task-specific MLPs: WIDAR (2-layer, 40% dropout), HugaDB (3-layer, 30% dropout with instance norm), and Stress Sensing (3-layer, batch norm). We apply an 80:20 train-test split per client and adapt benchmark models [63, 69, 82] for FL classification.

5.2 Evaluation on ***CurvFed***’s Effectiveness

To establish the effectiveness of ***CurvFed***, we have investigated the following research questions (RQs), each targeting a different aspect of fairness and efficacy in FL. The results addressing these questions are presented in corresponding evaluation tables as indicated below.

- **RQ-1:** Could ***CurvFed*** improve the fairness-efficacy balance compared to contemporary benign (i.e., non-fairness-aware) FL approaches or FWD FL baselines?
- **RQ-2:** Can fairness be achieved in FL settings that include both *single-person* and *multi-person* clients?
- **RQ-3:** Can ***CurvFed*** enhance fairness specifically for *single-person* clients?
- **RQ-4:** Could ***CurvFed*** improve fairness across *multiple sensitive attributes simultaneously*?

The following sections present a detailed analysis of each question.

5.2.1 RQ-1: Could *CurvFed*** improve the fairness-efficacy balance compared to contemporary benign FL approaches or FWD FL baselines?** We compare ***CurvFed*** against standard benign FL models—FedAvg, FedSAM, and FedSWA—and two recent fairness-without-disparity (FWD) approaches: KD-FedAvg [10] (adopted for FL settings) and FedSRCVaR [61]. Fairness is evaluated using the FATE score and Equal Opportunity (EO) gap with respect to *sex*.

FedAvg is the fairness-unaware baseline, while FedSAM and FedSWA are benign baselines that promote flatter loss landscapes via client-side SAM and server-side SWA [8].

Dataset	Model	F1 Score	EO Gap	FATE Score $\times 10^{-1}$
WIDAR	FedAvg	0.85	0.4263	0.0000
	FedSAM	0.8005	0.4251	-0.56
	FedSWA	0.8405	0.4071	0.33
	FedSRCVaR	0.7775	0.3828	0.160
	KD-Fedavg	0.8279	0.4097	0.122
	CurvFed	0.8100	0.3533	1.233
Stress sensing	FedAvg	0.7253	0.3069	0.0000
	FedSAM	0.7758	0.3034	0.812
	FedSWA	0.7406	0.3015	0.384
	FedSRCVaR	0.6692	0.2734	0.319
	KD-Fedavg	0.7154	0.2522	1.645
	CurvFed	0.7814	0.2522	2.559
HugaDB	FedAvg	0.8496	0.4369	0.0000
	FedSAM	0.8555	0.4255	0.329
	FedSWA	0.8418	0.4242	0.1917
	FedSRCVaR	0.8354	0.3939	0.815
	KD-Fedavg	0.8342	0.4166	0.281
	CurvFed	0.8855	0.3952	1.375

Table 1. Fairness–efficacy balance comparisons for RQ-1

FL Client composition reflecting real-world disparities: WIDAR and HugaDB clients typically include four males and one female (with one HugaDB client having two males and one female), while Stress Sensing shows greater variation (e.g., 2:4 to 3:6 male:female ratios). Unless otherwise noted, this distribution is used throughout.

Evaluation discussion: As shown in Table 1, **CurvFed** consistently improves the fairness–efficacy tradeoff. In WIDAR, it reduces the EO gap from 0.4263 (FedAvg) to 0.3533 with minimal F1 reduction (0.8100 vs. 0.8500). In Stress Sensing, it improves both F1 (0.7814 vs. 0.7253) and EO gap (0.2522 vs. 0.3069). HugaDB shows similar trends, with a higher F1 (0.8855) and reduced EO gap (0.3952) compared to FedAvg.

CurvFed consistently outperforms KD-FedAvg and FedSRCVaR in FATE scores across all datasets—Stress Sensing (2.559 vs. 1.645 and 0.319), WIDAR (1.233 vs. 0.122 and 0.160), and HugaDB (1.375 vs. 0.281 and 0.815). While KD-based methods excel in centralized settings with diverse group-wise data [10], their local fairness improvements do not reliably carry over after model aggregation in FL [29]. This limits their effectiveness in FL settings.

FedSRCVaR, relies on a constraint ρ to bound worst-case group sizes [61], assumes known group distributions—often unavailable in human-centric data with missing or highly variable groups across clients. This leads to unstable optimization and poor fairness–utility trade-off (e.g., F1 drops to 0.6692 in the Stress Sensing dataset). In contrast, **CurvFed** makes no such assumptions and achieves better fairness–performance balance.

5.2.2 RQ-2: Can fairness be achieved in FL settings that include both single-person and multi-person clients? Traditional fairness-aware FL methods assume each client contains data from all sensitive groups. However, as noted in Section 1 challenge 3, edge devices may contain data from a single user or multiple users. Thus, this assumption often fails in real-world deployments. Notably, **CurvFed** removes this assumption by promoting fairness through loss landscape regularization, making it impactful for practical deployment in human-sensing applications. Table 2 presents **CurvFed**’s performance across all three datasets, under a mix of single- and multi-person clients with 1–2 males and 0–1 females per client (See Appendix for detailed client distributions). Despite the absence of full group representation, **CurvFed** consistently outperforms other FL methods, achieving strong FATE scores of 0.770×10^{-1} (WIDAR), 4.604×10^{-1} (Stress Sensing), and 0.314×10^{-1} (HugaDB), demonstrating balanced fairness and performance under practical constraints.

5.2.3 *RQ-3: Can **CurvFed** enhance fairness specifically for single-person clients?* Only single-person clients are common in human-centric FL but pose challenges due to the lack of intra-client diversity, making global fairness and performance difficult to achieve. Prior studies [51, 83] show that simple aggregation methods like FedAvg often degrade global performance in these cases [51].

We evaluated **CurvFed** against other FWD baselines in only single-client scenarios. As shown in Table 2, **CurvFed** consistently achieves the best fairness-accuracy trade-off, with the highest FATE scores across all datasets: 0.601×10^{-1} for WIDAR, 3.511×10^{-1} for Stress Sensing, and 0.348×10^{-1} for HugaDB —demonstrating its effectiveness even without client-level sensitive attribute diversity.

Dataset	Client Type	Model	F1 Score	EO Gap	FATE Score $\times 10^{-1}$
WIDAR	Single & Multi-Person	FedAvg	0.8361	0.4289	0.0000
		FedSAM	0.8311	0.4122	0.329
		FedSWA	0.8540	0.4366	0.0364
		KD-FedAvg	0.7844	0.4085	-0.140
		FedSRCVaR	0.7105	0.4085	-1.024
		CurvFed	0.7938	0.3742	0.770
	Single Person Only	FedAvg	0.8420	0.4302	0.0000
Stress Sensing	Single & Multi-Person	FedSAM	0.8383	0.4148	0.313
		FedSWA	0.8421	0.4289	0.0321
		FedSRCVaR	0.7064	0.4149	-1.253
		KD-FedAvg	0.7691	0.4097	-0.389
		CurvFed	0.7998	0.3828	0.601
	Single Person Only	FedAvg	0.7542	0.3774	0.0000
		FedSAM	0.7467	0.3877	-0.371
		FedSWA	0.8350	0.3121	2.802
		KD-FedAvg	0.7471	0.2487	3.318
		FedSRCVaR	0.6967	0.2751	1.948
HugaDB	Single & Multi-Person	CurvFed	0.8300	0.2416	4.604
		FedAvg	0.7607	0.3827	0.0000
		FedSAM	0.7663	0.3395	1.204
		FedSWA	0.7820	0.3633	0.786
		FedSRCVaR	0.6757	0.2222	3.076
	Single Person Only	KD-FedAvg	0.6764	0.2522	2.303
		CurvFed	0.7298	0.2328	3.511
		FedAvg	0.8610	0.4380	0.0000
		FedSAM	0.8480	0.4142	0.293
		FedSWA	0.8404	0.4107	0.287

Table 2. Performance comparison across different client setups: single & multi-person clients (RQ2) and single-person clients (RQ3)

5.2.4 *RQ-4: Could **CurvFed** improve fairness across multiple sensitive attributes simultaneously?* In FL-based human sensing, data often simultaneously involve multiple sensitive attributes (e.g., sex, age, body type, sensor placement). To assess **CurvFed** under such conditions, we evaluated fairness with respect to additional sensitive attributes—hands' (watch-hand) and orientation' (sensor placement)—in the Stress Sensing and WIDAR datasets, using the same models as in Table 1. For WIDAR, we induced disparity by subsampling 50% of data from orientations 4 and 5, grouping orientations 1–3 as "major" and the rest as "minor." In Stress Sensing, only 13 of 48

Dataset	Sensitive Attribute	Model	F1 Score	EO Gap	FATE Score $\times 10^{-1}$
WIDAR	Orientation	FedAvg	0.8436	0.5130	0.0000
		FedSAM	0.8007	0.5082	-0.414
		FedSWA	0.8494	0.5146	0.037
		FedSRCVaR	0.7772	0.4318	0.795
		KD-Fedavg	0.8279	0.4756	0.543
		CurvFed	0.8100	0.3814	2.154
Stress Sensing	Hand	FedAvg	0.7253	0.4797	0.0000
		FedSAM	0.7758	0.4268	1.799
		FedSWA	0.7406	0.4638	0.928
		FedSRCVaR	0.6692	0.3651	1.617
		KD-Fedavg	0.7154	0.3957	1.615
		CurvFed	0.7814	0.4320	1.766

Table 3. Performance metrics comparison under different sensitive attributes for RQ4

participants had both-hand data, while others had left-hand only. HugaDB, with only sex as a sensitive attribute, was excluded.

As shown in Table 3, **CurvFed** achieves strong FATE scores across sensitive attributes, underscoring its effectiveness in enhancing fairness while maintaining competitive accuracy. Although **FedSAM** slightly outperforms others in Stress Sensing with **CurvFed** being second best. Notably, both the approaches target the loss landscape curvature attributes [25]. **CurvFed** delivers the highest FATE score on WIDAR. These results highlight **CurvFed**'s capability to effectively balance fairness and accuracy, thereby addressing Challenge 4 from Section 1.

5.3 Feasibility Study

This section presents a comprehensive set of experiments to evaluate the real-world feasibility of **CurvFed**.

Client	Device	Training Time (s)	Memory (MB)	Train Usage (%)	Upload Time (s)
Client 1	Google Pixel 6	0.7819	268.48	27.65	3.48
Client 2	Google Pixel 6	0.525	267.88	28.63	4.03
Client 3	Raspberry Pi 5	0.4732	281.36	41.92	3.20
Client 4	Intel i5-14600T	0.206	256.80	3.34	3.39
Client 5	Intel i5-14600T	0.239	259.69	2.45	3.48
Client 6	Jetson Nano	0.409	288.27	7.54	1.903

Table 4. Per-client training statistics from the real-world FL deployment. Metrics include training time, Process RSS memory usage (MB), average CPU utilization, and model upload latency.

5.3.1 Feasibility of Real-World Deployment with CurvFed: To evaluate the real-world deployability of **CurvFed**, we conducted a live FL deployment using a heterogeneous set of six edge devices: two Google Pixel 6 smartphones, a Raspberry Pi 5, an NVIDIA Jetson Nano, and two Intel i5-14600T desktops (Fig. 2). Each device was assigned data from a unique participant in the Stress Sensing dataset (Section 5.1) and exchanged model updates with a central server via Google Cloud APIs authenticated through PyDrive.

Table 4 summarizes training time, memory usage, CPU utilization, and upload latency for each client (and across devices). Desktops were fastest; Pixel 6 and Raspberry Pi showed moderate resource use; Jetson Nano balanced performance and efficiency. Consistent upload times confirmed stable communication, supporting **CurvFed**'s real-world deployability on edge platforms.

To complement the real-world study, we benchmarked **CurvFed** against standard FL baselines (FedAvg, FedSAM) on *seven* deployment platforms—from high-performance GPUs (NVIDIA RTX 4090) to resource-constrained devices (Raspberry Pi 5, Pixel 6) to assess real-world feasibility. Across five runs using the WIDAR dataset, we

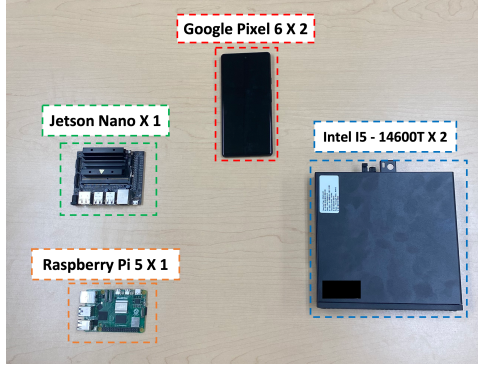


Fig. 2. Experimental setup for real-world FL evaluation using heterogeneous edge devices.

measured training time, memory usage, resource utilization, and inference time on average. As shown in Table 5, **CurvFed** incurs moderate training overhead due to the Fisher penalty, similar to FedSAM’s cost for sharpness-aware updates. However, this overhead is practical—even on edge devices—and does not affect inference time. Methods like FedSWA and FedSRCVaR were excluded as their client-side costs mirror FedAvg, with additional computations handled server-side. Overall, **CurvFed** demonstrates efficiency and feasibility across heterogeneous edge devices.

Platform	Approach	Train (s)	RSS (MBs)	Infer (s)	Train Usage (%)
Intel i9-9900K Processor	Fedavg	1.67	1074.05	0.03	48.12
	FedSAM	5.78	1147.54	0.02	48.07
	CurvFed	9.34	1287.87	0.02	48.134
AMD Ryzen 9 7950X 16-Core Processor	Fedavg	0.77	1033.62	0.01	24.93
	FedSAM	3.23	1109.04	0.01	24.30
	CurvFed	5.42	1420.88	0.01	24.52
Apple M1	Fedavg	4.02	418.916	0.16	1.05
	FedSAM	8.95	450.31	0.16	1.06
	CurvFed	11.53	387.36	0.16	1.00
Quadro RTX 5000	Fedavg	0.73	961.77	0.01	46.4
	FedSAM	0.81	1070.73	0.01	73.0
	CurvFed	1.04	1176.54	0.01	62.3
NVIDIA GeForce RTX 4090	Fedavg	0.14	954.52	0.01	15.0
	FedSAM	0.18	1063	0.01	49.1
	CurvFed	0.32	1290.88	0.01	48.6
Google Pixel 6	Fedavg	4.24	370.84	0.12	49.11
	FedSAM	13.39	337.40	0.12	49.11
	CurvFed	26.59	326.28	0.20	49.07
Raspberry Pi 5	Fedavg	13.5	518.88	0.21	48.79
	FedSAM	40.8	489	0.23	48.7
	CurvFed	56.4	490	0.22	49

Table 5. Training Time (s), Training Process (RSS) Memory Usage (MBs), Inference Time (s), Training Resource usage (%) for FL Approaches across Different Platforms

5.3.2 Communication Overhead: We compare **CurvFed**’s communication cost with FL baselines: Fedavg, KD-Fedavg and FedSWA approaches exchange 34.38MB (WIDAR) and 0.042MB (Stress Sensing) per round. As

overhead, **CurvFed** adds only 8 bytes for sharpness-aware aggregation, while FedSRCVaR adds 4 bytes for a risk threshold—both negligible relative to their fairness benefits.

5.3.3 Resource Utilization and Overhead Breakdown. We measured the per-batch average training time and Fisher top-eigenvalue computation time (averaged over five runs) across all our evaluation platforms using a single client from the WIDAR dataset. Results are summarized in Table 6. While Fisher computation introduces additional cost (typically $\sim 30\text{--}40\%$ of per-batch training time), the absolute time per call remains modest (milliseconds on GPUs and tens to hundreds of milliseconds on CPUs and mobile devices). These measurements indicate that Fisher overhead scales proportionally with device compute capability and remains practical within the constraints of on-device FL training.

Platform	Avg. Train Time / batch (s)	Avg. Fisher Time / batch (s)
GPU: Quadro RTX 5000	0.027	0.010
GPU: NVIDIA RTX 4090	0.003	0.001
CPU: AMD Ryzen 9 7950X	0.076	0.029
Apple M1	0.298	0.137
Pixel 6: Cortex-A55	0.355	0.146
CPU: Intel i9-9900K	0.169	0.062
CPU: Intel i5-14600T	0.268	0.175
Jetson Nano: Cortex-A57	1.040	0.393
Raspberry Pi: Cortex-A76	1.621	0.733

Table 6. Average per-batch training time and Fisher computation time across platforms.

To contextualize these results, we also benchmarked the upload and download latency for a trained model (~ 34.4 MB) across CPU-based platforms, using Google Cloud APIs with PyDrive authentication (Table 7). Communication latency per round is on the order of *seconds*, which is *one to two orders of magnitude higher than the Fisher computation overhead per batch*. Since such communication is repeated across many FL rounds (e.g., 80 rounds for WIDAR), network transfer typically dominates the end-to-end runtime [40].

Platform	File Size (MB)	Upload (s)	Download (s)
CPU: AMD Ryzen 9 7950X	34.39	2.30	6.42
Jetson Nano: Cortex-A57	34.39	2.83	4.43
Raspberry Pi: Cortex-A76	34.39	2.42	3.96
CPU: Intel i5-14600T	34.39	3.32	3.80
Pixel 6: Cortex-A55	34.39	5.05	4.73
CPU: Intel i9-9900K	34.39	2.36	5.41

Table 7. Upload and download latency for a trained model (~ 34.4 MB) across CPU platforms.

These experiments suggest that while Fisher computation contributes a consistent overhead during local training, communication latency remains the dominant factor in federated learning deployments [40, 97]. This indicates that curvature-based regularization is computationally feasible in practice [37], with networking emerging as the primary bottleneck. Exploring lighter curvature proxies [77] and adaptive scheduling [92] remains a valuable direction for further improving scalability.

5.4 Sensitivity Analysis

In this section, we explore the performance and practicality of **CurvFed** under the following real-world scenarios:

- (1) Effect of Ordered Sampling on FL Performance
- (2) Effect of Subsampling Local Labeled Data and Clients on Global Fairness
- (3) Impact of Random Client Participation on Fairness Across Models

Here, we focus on the WIDAR and Stress Sensing datasets using *sex* as the sensitive attribute. They were chosen for their contrasting modalities: WIDAR is uni-modal, while Stress Sensing is multi-modal. While FedSAM and FedSWA were previously compared for benign generalization, they are excluded here to emphasize fairness-oriented baselines: FedAvg serves as the primary benign baseline, and KD-FedAvg and FedSRCVaR serve as FWD FL baselines.

5.4.1 Effect of Ordered Sampling on FL Performance: Human-sensing data often contains strong temporal dependencies [47, 52], making it important to preserve data order during local training [50, 53]. It also mimics real-world FL deployments [78]. To reflect this, we evaluate FL performance using an ordered 80:20 train-test split without shuffling. As shown in Table 8, **CurvFed** achieves the best fairness–utility tradeoff, reducing the EO gap and achieving the highest F1 and FATE scores, demonstrating its effectiveness in temporally structured FL settings.

Dataset	Model	F1 Score	EO Gap	FATE Score $\times 10^{-1}$
WIDAR	FedAvg	0.8570	0.4629	0.0000
	FedSRCVaR	0.7676	0.4002	0.311
	KD-FedAvg	0.8135	0.4069	0.701
	CurvFed	0.7488	0.3452	1.280
Stress Sensing	FedAvg	0.7482	0.4000	0.0000
	FedSRCVaR	0.6989	0.3633	0.259
	KD-FedAvg	0.7326	0.3633	0.709
	CurvFed	0.7693	0.2938	2.935

Table 8. Comparison of model performance under ordered 80:20 splits to capture temporal dependencies

5.4.2 Effect of Subsampling of Local Labeled Data and Clients on Global Fairness: In real-world edge deployments, clients often operate under resource constraints, leading to limited local data and sporadic client availability [43]. To simulate this, we evaluate **CurvFed** under (i) varying local training data availability (20%, 50%, 90%), and (ii) fluctuating client participation per round (3, 5, 7 clients), with a fixed 20% test set.

As shown in Figs. 3 and 4, **CurvFed** consistently demonstrates competitive or superior performance in terms of both fairness (lower EO gap) and utility (higher FATE score) across the WIDAR and Stress Sensing datasets. Notably, in low-data regimes (e.g., 20%), **CurvFed** maintains a clear advantage over FedAvg and KD, while FedSRCVaR occasionally achieves lower EO gaps but with significant sacrifices in FATE scores—especially evident in the WIDAR dataset with 3 and 5 clients. Furthermore, CurvFed’s performance stabilizes with $\geq 50\%$ data, suggesting robustness even with moderate training data. In client subsampling scenarios, CurvFed maintains the best fairness–utility balance across different client counts, indicating its suitability for dynamic, resource-constrained FL deployments.

5.4.3 Impact of Random Client Participation on Fairness: In real-world FL deployments, especially in human-sensing applications, client availability is often inconsistent due to network instability and device constraints [49]. Unlike idealized settings with fixed clients per round, edge devices may randomly join or drop out during training. We simulate this, where clients were independently sampled using Bernoulli sampling with each client having a random probability (ranging from 0.1 to 0.9) of getting selected, introducing realistic variations in both the number and identity of participating clients.

Despite this variability, **CurvFed** consistently achieves the best fairness–accuracy tradeoff, achieving the highest FATE scores—while also attaining the lowest EO gaps, as shown in Fig. 5. While FedSRCVaR sometimes matches fairness, it sacrifices accuracy, and KD-FedAvg shows unstable results. These results demonstrate **CurvFed**’s robustness to client variability in practical FL deployments.

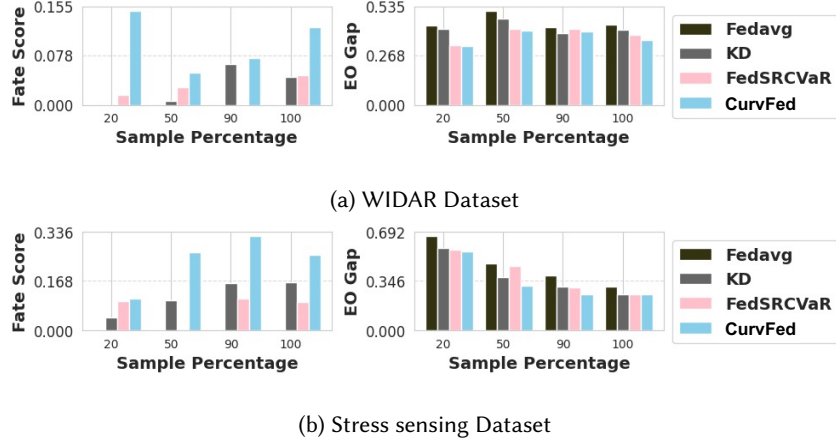


Fig. 3. Impact of limited local data availability (20%, 50%, 90%) on fairness and utility in FL

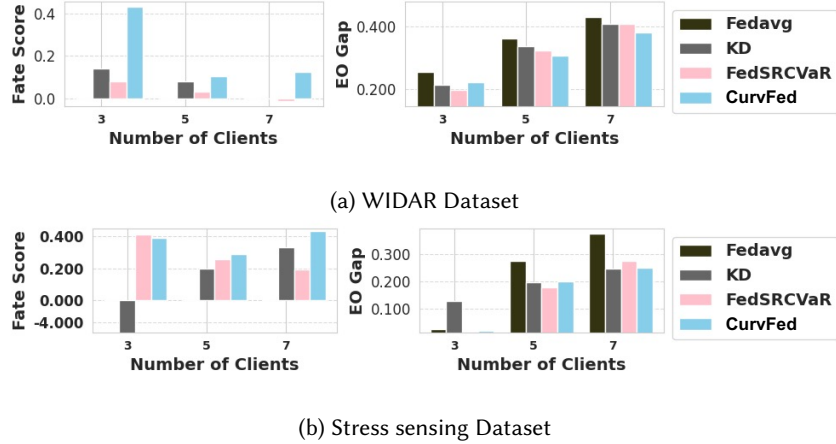


Fig. 4. Impact of client participation subsampling (3 or 5 or 7 clients per round) on fairness-utility trade-off

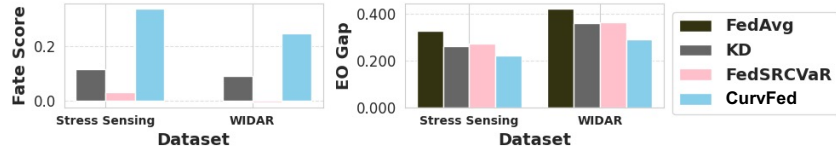


Fig. 5. Experiment on real-world FL evaluation simulating an inconsistent number of clients in each round.

5.5 Ablation Study

To validate the design choices of our proposed **CurvFed** framework, we conducted an extensive ablation study, detailed in Appendix. This study systematically isolates and evaluates the independent contributions of three key components: (1) the *sharpness-aware aggregation strategy*, (2) the *sharpness-aware client-side training with fairness constraints*, and (3) the use of the *top eigenvalue of FIM penalty* as a regularization term.

5.5.1 Independent Effect of Sharpness-Aware Aggregation: We evaluated three aggregation strategies: based on classification loss, based on the top eigenvalue of the Fisher Information Matrix (FIM), and one that combines both via soft weighting—without applying FIM regularization during local client training. The combined approach consistently improved both fairness and accuracy across datasets, with an average EO Gap reduction of 6.78% compared to FedAvg, highlighting the standalone effectiveness of sharpness-aware aggregation.

5.5.2 Independent Effect of Sharpness-Aware Client-Side Training: We applied the FIM top eigenvalue penalty during local client training while using a benign server-side aggregation strategy. This alone improved fairness, reducing the EO gap by an average of 6.60% compared to benign Fedavg across all three datasets, confirming the standalone benefit of sharpness-aware local training.

5.5.3 Effect of Top eigenvalue of FIM and SAM. We examined the impact of combining the client-side *FIM top eigenvalue* penalty with sharpness-aware aggregation and SAM. The results show:

- The FIM penalty improves fairness but may slightly reduce accuracy.
- SAM enhances model accuracy but slightly reduces fairness.
- Combining the FIM penalty with sharpness-aware aggregation (without SAM) yields a better fairness-accuracy trade-off, though at a slight cost to accuracy.

5.5.4 Effectiveness of complete CurvFed Integration: The full **CurvFed** configuration—integrating SAM, FIM top eigenvalue regularization, and sharpness-aware aggregation—achieves the best overall trade-off between fairness and efficacy. It consistently outperforms other variations across all datasets in terms of both EO Gap and F1 score, supporting the effectiveness of the complete approach described in Algorithm 1.

6 Empirical Justification

While Section 5 confirms the effectiveness of **CurvFed**, this section offers an empirical justification of *why and how* it works. Specifically, we empirically evaluate whether the observed outcomes support the propositions introduced in Section 3.2, which hypothesize the mechanisms through which CurvFed improves fairness and performance in the absence of sensitive attributes. Each of the following subsections corresponds to one of the three propositions and presents analysis and visualizations using the WIDAR and stress sensing datasets.

(Validation of P1) Alignment between FIM and Hessian top eigenvalue: Fig. 6 illustrates the relationship between communication rounds and test-set model performance in terms of the FATE Score, F1 Score, and Loss Landscape, for the Stress Sensing dataset and WIDAR dataset. We utilized FATE score as our selection criterion for the best global model highlighted in yellow, corresponding to round 20.

Fig. 7 shows the mean per-person top eigenvalues of the Hessian and FIM for the Stress Sensing in Fig. 7 (a) and WIDAR dataset in Fig. 7 (b). Notably, the graph traits for both FIM and Hessian are similar, and lowest in our optimal selected round (20), providing empirical justification for *proposition 1*.

(Validation of P2) Minimizing the FIM Top Eigenvalue Reduces group Curvature Disparity: To evaluate whether FL training aligns with proposition 2 discussed in Section 3.2, we analyze the difference in curvature metrics across known sensitive attribute groups. Table 9 reports the difference in the top eigenvalues (λ) of the FIM and Hessian matrix for the sensitive attribute *sex* across two distributions, $D_{\text{male}}^{\text{sex}}$ and $D_{\text{female}}^{\text{sex}}$ along with the FATE scores for the WIDAR and Stress sensing datasets.

Global Trends: FedSAM and FedSWA reduce curvature disparity via implicit sharpness minimization at the client and server levels, respectively. While this results in moderate gains in both curvature alignment and FATE scores, **CurvFed** consistently outperforms them in curvature alignment and FATE scores, confirming the superior effectiveness of explicit FIM-based sharpness regularization.

Client-Level Trends: Does CurvFed Reduce group-wise Disparity Locally? To examine whether global fairness trends extend to individual clients, we visualize group-wise FIM eigenvalues for randomly selected clients from

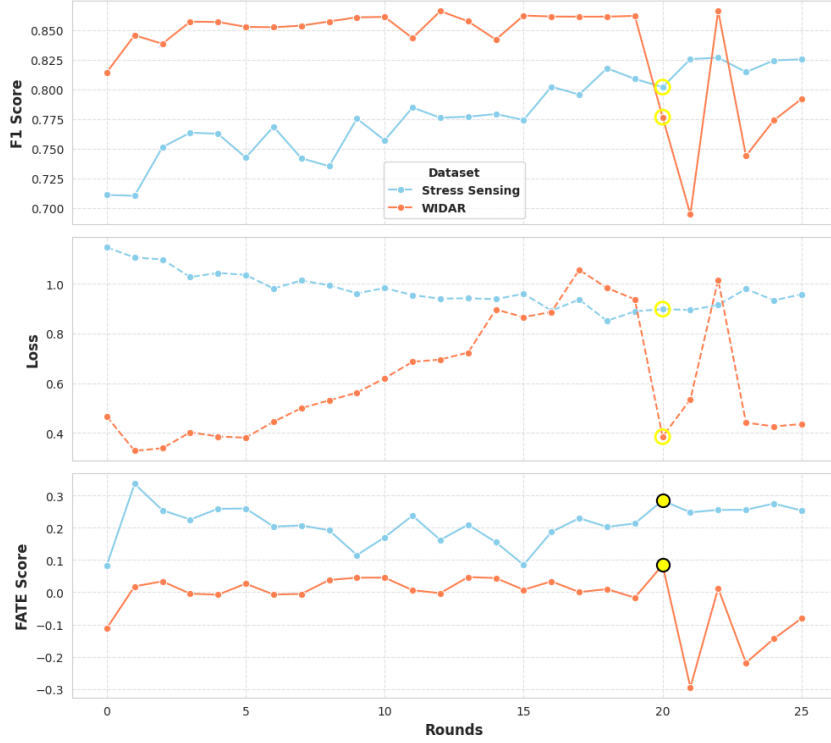


Fig. 6. FATE score, F1 score, and loss landscape across communication rounds for **CurvFed** on Stress Sensing and WIDAR datasets

Dataset	Model	$\Delta\lambda(\mathbf{F})$	$\Delta\lambda(\mathbf{H})$	FATE Score $\times 10^{-1}$
WIDAR	Fedavg	0.009	0.061	0.0000
	FedSAM	0.009	0.0365	-0.56
	FedSWA	0.002	0.019	0.33
	FedSRCVaR	0.0015	0.0310	0.160
	KD-Fedavg	0.0022	0.0377	0.122
	CurvFed	0.0007	0.0017	1.233
Stress Sensing	Fedavg	0.03	0.0330	0.0000
	FedSAM	0.019	0.0347	0.812
	FedSWA	0.020	0.0278	0.38
	FedSRCVaR	0.019	0.1446	0.319
	KD-Fedavg	0.021	0.6089	1.645
	CurvFed	0.004	0.0097	2.559

Table 9. Disparity based on ‘Sex’ Across Datasets for Different Models

the Stress Sensing dataset (see Fig. 8). We analyze changes across sensitive attributes such as *sex* and *handedness* before and after local training.

The visualizations show that reducing the top eigenvalue of the FIM not only lowers overall curvature but also reduces disparity between groups at the client level—supporting our *proposition 2*.

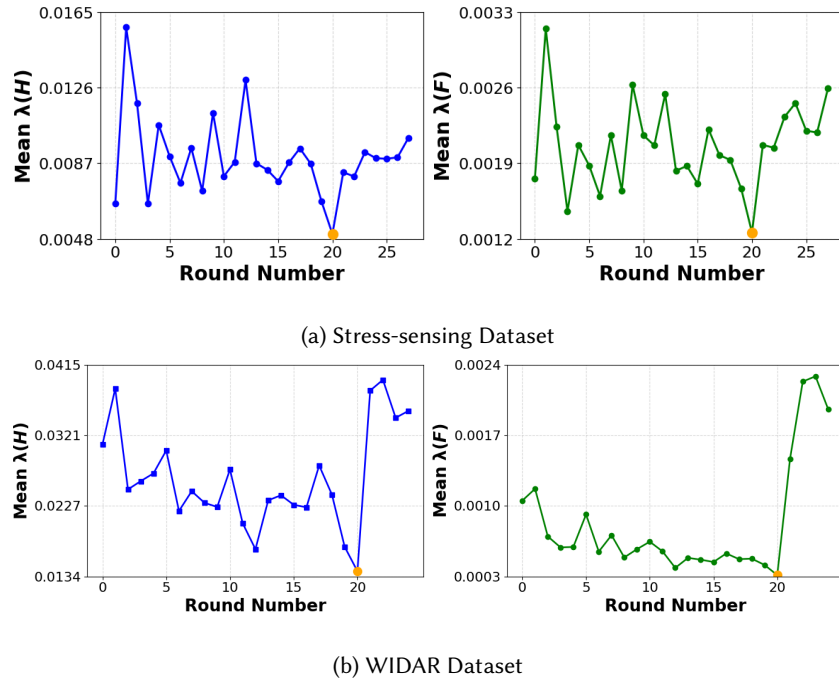
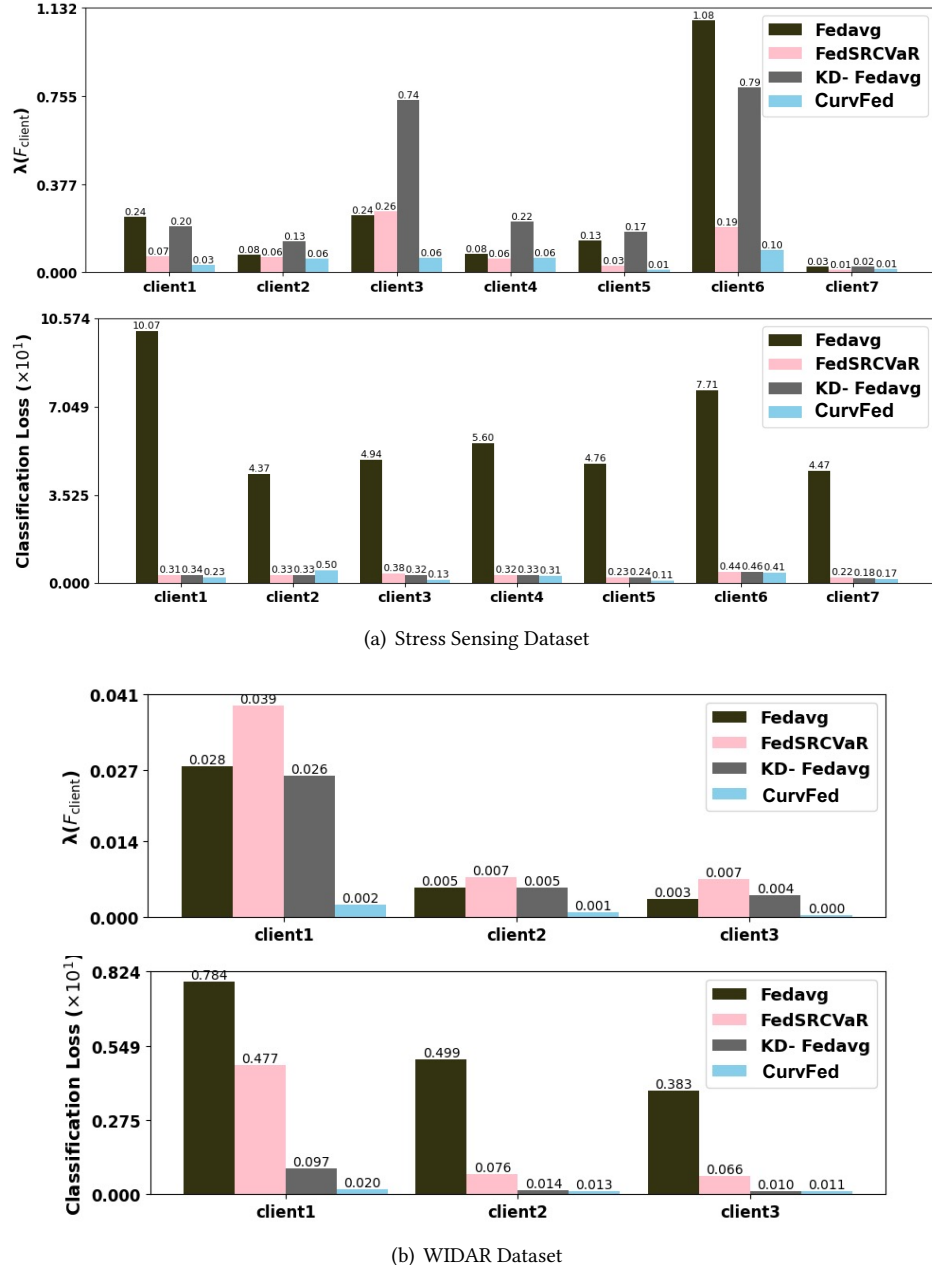


Fig. 7. Comparison of Mean Person-wise top eigenvalues for Hessian and Fisher matrices across Rounds



Fig. 8. Top eigenvalue of Fisher matrix by Sex and Hand across different clients and rounds in Stress Sensing Dataset.

(Validation of P3) Sharpness-Aware Aggregation Reduces Variance in Excessive Loss Across Clients: To verify whether *CurvFed* indeed upholds this proposition, we visualized the $\lambda(F_{client})$ and classification loss among single-person and multi-person clients in FL systems for WIDAR and Stress-Sensing datasets, as shown in Fig. 9. *CurvFed* outperforms other FWD baselines by consistently reducing variance across the excessive loss in the form of ‘reducing variances across the top eigenvalue values $\lambda(F)$ and loss’ across clients. *This visualization confirms proposition 3.*

Fig. 9. Client-wise comparison of maximum Fisher eigenvalue $\lambda(F_{\text{client}})$ and classification loss across different models

7 Broader Impact and Limitation

This first-of-its-kind paper bridges the gap between fairness and federated learning in human-sensing applications, paving the way for a more equitable and responsible future in decentralized human-sensing, ensuring fair access to technological advancements for all. *Some limitations and future research scopes are discussed below:*

- Achieving fairness in FL systems requires attaining a balance between fairness and model performance [27]. The quest to ensure fairness for individual clients often results in reduced performance across the board, an issue highlighted in literature [4, 23, 75, 89]. Although **CurvFed** demonstrates significant effectiveness in achieving this balance, as discussed in Section 5.2, **RQ-3**, it exhibits minor performance degradation in the WIDAR and Stress sensing dataset for single-person clients. This could be attributed to our aggregation scheme, outlined in Section 4.1 Equation 12, which equally weighs low error rates and lower maximal uncertainty, thus limiting the ability to balance accuracy and fairness when dealing with single-person clients. The issue could be resolved by introducing a hyperparameter as the weighting factor.
- Recent studies have explored the relationship between fairness and privacy in machine learning, often treating them as competing metrics [72, 91]. While this work has focused on fairness in FL, extending the investigation to explore the interplay between fairness and privacy in FL would be an important direction for future research.
- A limitation of our study is the experimental scale, constrained by the lack of large-scale human-sensing datasets with sensitive attributes. While prior (non-human-centric) FL fairness works often evaluate on a larger number of clients, such datasets remain scarce in the human sensing domain [85]. Even recent large-scale datasets like GLOBEM [80] do not release demographic or other sensitive information needed for fairness evaluation. This gap has also been discussed in recent survey studies within the ubiquitous sensing community [84, 86].
- Like many Rawlsian or min-max fairness approaches [30, 39], **CurvFed** promotes equity by aligning loss landscape curvatures across clients, which prioritizes worst-case (or underrepresented) groups. This strategy can occasionally come at the expense of performance in majority groups, a trade-off that has also been reported in other fairness-driven FL methods [20, 57, 60]. While this reflects a broader property of parity-based optimization [26, 59] rather than a limitation of **CurvFed** itself, it highlights an important avenue for future research: designing FWD mechanisms that uplift the worst-off groups without diminishing performance for others, thereby moving toward Pareto-improving fairness [58, 87].

8 Conclusion

This paper presents **CurvFed**, a novel fairness-enhancing strategy for FL that introduces sharpness-aware regularization during local training and aggregation. Unlike existing methods, **CurvFed** is theoretically grounded and operates without access to sensitive or bias-inducing attributes, thereby preserving FL’s core privacy principles. Extensive evaluations—including a live real-world deployment on heterogeneous, resource-constrained edge devices—demonstrate **CurvFed**’s effectiveness in achieving a strong fairness–performance trade-off across diverse human-sensing applications, even under single- or multi-user scenarios with multiple unknown bias sources. Ablation studies and empirical justifications further validate that leveraging loss-landscape sharpness is key to improving fairness. Overall, **CurvFed** offers a practical and privacy-respecting path forward for equitable FL in real-world human-sensing systems.

References

- [1] ABAY, A., ZHOU, Y., BARACALDO, N., RAJAMONI, S., CHUBA, E., AND LUDWIG, H. Mitigating bias in federated learning. *arXiv preprint arXiv:2012.02447* (2020).
- [2] ABBAS, Q., MALIK, K. M., SAUDAGAR, A. K. J., AND KHAN, M. B. Context-aggregator: An approach of loss-and class imbalance-aware aggregation in federated learning. *Computers in Biology and Medicine* 163 (2023), 107167.

- [3] AKIBA, T., SANO, S., YANASE, T., OHTA, T., AND KOYAMA, M. Optuna: A next-generation hyperparameter optimization framework. In *Proceedings of the 25th ACM SIGKDD international conference on knowledge discovery & data mining* (2019), pp. 2623–2631.
- [4] AL AMIN, M. T., ABDELZAHER, T., WANG, D., AND SZYMANSKI, B. Crowd-sensing with polarized sources. In *2014 IEEE International Conference on Distributed Computing in Sensor Systems* (2014), IEEE, pp. 67–74.
- [5] ARCURI, A., AND DARI-MATTIACCI, G. Centralization versus decentralization as a risk-return trade-off. *The Journal of Law and Economics* 53, 2 (2010), 359–378.
- [6] BOYD, S. P., AND VANDENBERGHE, L. *Convex optimization*. Cambridge university press, 2004.
- [7] BRYNJOLFSSON, E., AND NG, A. Big ai can centralize decision-making and power, and that'sa problem. *Missing links in AI governance* (2023), 65–87.
- [8] CALDAROLA, D., CAPUTO, B., AND CICCONE, M. Improving generalization in federated learning by seeking flat minima. In *European Conference on Computer Vision* (2022), Springer, pp. 654–672.
- [9] CASTELNOVO, A., CRUPI, R., GRECO, G., REGOLI, D., PENCO, I. G., AND COSENTINI, A. C. A clarification of the nuances in the fairness metrics landscape. *Scientific Reports* 12, 1 (2022), 4209.
- [10] CHAI, J., JANG, T., AND WANG, X. Fairness without demographics through knowledge distillation. *Advances in Neural Information Processing Systems* 35 (2022), 19152–19164.
- [11] CHEN, H., ZHU, T., ZHANG, T., ZHOU, W., AND YU, P. S. Privacy and fairness in federated learning: on the perspective of trade-off. *ACM Computing Surveys* (2023).
- [12] CHERESHNEV, R., AND KERTÉSZ-FARKAS, A. Hugadb: Human gait database for activity recognition from wearable inertial sensor networks. In *Analysis of Images, Social Networks and Texts: 6th International Conference, AIST 2017, Moscow, Russia, July 27–29, 2017, Revised Selected Papers* 6 (2018), Springer, pp. 131–141.
- [13] CHIU, C.-H., CHEN, Y.-J., WU, Y., SHI, Y., AND HO, T.-Y. Achieve fairness without demographics for dermatological disease diagnosis. *Medical Image Analysis* 95 (2024), 103188.
- [14] COTTER, A., GUPTA, M., JIANG, H., SREBRO, N., SRIDHARAN, K., WANG, S., WOODWORTH, B., AND YOU, S. Training fairness-constrained classifiers to generalize. In *ICML 2018 workshop:“fairness, accountability, and transparency in machine learning (FAT/ML)* (2018).
- [15] CUI, S., PAN, W., LIANG, J., ZHANG, C., AND WANG, F. Addressing algorithmic disparity and performance inconsistency in federated learning. *Advances in Neural Information Processing Systems* 34 (2021), 26091–26102.
- [16] DAUPHIN, Y. N., AGARWALA, A., AND MOBAHI, H. Neglected hessian component explains mysteries in sharpness regularization. *arXiv preprint arXiv:2401.10809* (2024).
- [17] DJEBROUNI, Y. Towards bias mitigation in federated learning. In *16th EuroSys Doctoral Workshop* (2022).
- [18] DJEBROUNI, Y., BENARBA, N., TOUAT, O., DE ROSA, P., BOUCHENAK, S., BONIFATI, A., FELBER, P., MARANGOZOVA, V., AND SCHIAVONI, V. Bias mitigation in federated learning for edge computing. *Proceedings of the ACM on Interactive, Mobile, Wearable and Ubiquitous Technologies* 7, 4 (2024), 1–35.
- [19] DONG, X., CHEN, S., AND PAN, S. Learning to prune deep neural networks via layer-wise optimal brain surgeon. *Advances in neural information processing systems* 30 (2017).
- [20] DU, W., XU, D., WU, X., AND TONG, H. Fairness-aware agnostic federated learning. In *Proceedings of the 2021 SIAM International Conference on Data Mining (SDM)* (2021), SIAM, pp. 181–189.
- [21] DWORK, C., HARDT, M., PITASSI, T., REINGOLD, O., AND ZEMEL, R. Fairness through awareness. In *Proceedings of the 3rd innovations in theoretical computer science conference* (2012), pp. 214–226.
- [22] EPSTEIN, D. A., CALDEIRA, C., FIGUEIREDO, M. C., LU, X., SILVA, L. M., WILLIAMS, L., LEE, J. H., LI, Q., AHUJA, S., CHEN, Q., ET AL. Mapping and taking stock of the personal informatics literature. *Proceedings of the ACM on Interactive, Mobile, Wearable and Ubiquitous Technologies* 4, 4 (2020), 1–38.
- [23] EZZELDIN, Y. H., YAN, S., HE, C., FERRARA, E., AND AVESTIMEHR, A. S. Fairfed: Enabling group fairness in federated learning. In *Proceedings of the AAAI Conference on Artificial Intelligence* (2023), vol. 37, pp. 7494–7502.
- [24] FERRY, J., AIVODJI, U., GAMBS, S., HUGUET, M.-J., AND SIALA, M. Improving fairness generalization through a sample-robust optimization method. *Machine Learning* 112, 6 (2023), 2131–2192.
- [25] FORET, P., KLEINER, A., MOBAHI, H., AND NEYSHABUR, B. Sharpness-aware minimization for efficiently improving generalization. In *International Conference on Learning Representations* (2021).
- [26] FOULDS, J. R., AND PAN, S. Are parity-based notions of {AI} fairness desirable? *A Quarterly bulletin of the Computer Society of the IEEE Technical Committee on Data Engineering* 43, 4 (2020).
- [27] GU, X., TIANQING, Z., LI, J., ZHANG, T., REN, W., AND CHOO, K.-K. R. Privacy, accuracy, and model fairness trade-offs in federated learning. *Computers & Security* 122 (2022), 102907.
- [28] GUO, Y., LIN, T., AND TANG, X. Towards federated learning on time-evolving heterogeneous data. *arXiv preprint arXiv:2112.13246* (2021).
- [29] HAMMAN, F., AND DUTTA, S. Demystifying local and global fairness trade-offs in federated learning using partial information decomposition. *arXiv preprint arXiv:2307.11333* (2023).
- [30] HASHIMOTO, T., SRIVASTAVA, M., NAMKOONG, H., AND LIANG, P. Fairness without demographics in repeated loss minimization. In

International Conference on Machine Learning (2018), PMLR, pp. 1929–1938.

[31] HORN, R. A., AND JOHNSON, C. R. *Matrix analysis*. Cambridge university press, 2012.

[32] HOUSE, T. W. Removing barriers to american leadership in artificial intelligence. *Executive Order* 23 (2025).

[33] IZMAILOV, P., PODOPRIKHIN, D., GARIFOV, T., VETROV, D., AND WILSON, A. G. Averaging weights leads to wider optima and better generalization. *arXiv preprint arXiv:1803.05407* (2018).

[34] JASTRZĘBSKI, S., KENTON, Z., BALLAS, N., FISCHER, A., BENGIO, Y., AND STORKEY, A. On the relation between the sharpest directions of dnn loss and the sgd step length. *arXiv preprint arXiv:1807.05031* (2018).

[35] JUI, T. D., AND RIVAS, P. Fairness issues, current approaches, and challenges in machine learning models. *International Journal of Machine Learning and Cybernetics* (2024), 1–31.

[36] KAUR, M. Wireless sensor networks: Issues & challenges.

[37] KHAN, K., GOODRIDGE, W., AND ELIBOX, W. A functional rna-based and curvature-aware learning framework for federated optimization. *Neurocomputing* (2025), 131045.

[38] KIM, Y.-H., JEON, J. H., CHOE, E. K., LEE, B., KIM, K., AND SEO, J. Timeaware: Leveraging framing effects to enhance personal productivity. In *Proceedings of the 2016 CHI Conference on Human Factors in Computing Systems* (2016), pp. 272–283.

[39] LAHOTI, P., BEUTEL, A., CHEN, J., LEE, K., PROST, F., THAIN, N., WANG, X., AND CHI, E. Fairness without demographics through adversarially reweighted learning. *Advances in neural information processing systems* 33 (2020), 728–740.

[40] LE, K., LUONG-HA, N., NGUYEN-DUC, M., LE-PHUOC, D., DO, C., AND WONG, K.-S. Exploring the practicality of federated learning: A survey towards the communication perspective. *arXiv preprint arXiv:2405.20431* (2024).

[41] LEE, B.-K., KIM, J., AND RO, Y. M. Masking adversarial damage: Finding adversarial saliency for robust and sparse network. In *Proceedings of the IEEE/CVF Conference on Computer Vision and Pattern Recognition* (2022), pp. 15126–15136.

[42] LEE, H., AHN, C. R., CHOI, N., KIM, T., AND LEE, H. The effects of housing environments on the performance of activity-recognition systems using wi-fi channel state information: An exploratory study. *Sensors* 19, 5 (2019), 983.

[43] LI, A., SUN, J., ZENG, X., ZHANG, M., LI, H., AND CHEN, Y. Fedmask: Joint computation and communication-efficient personalized federated learning via heterogeneous masking. In *Proceedings of the 19th ACM Conference on Embedded Networked Sensor Systems* (2021), pp. 42–55.

[44] LI, C., CAO, Z., AND LIU, Y. Deep ai enabled ubiquitous wireless sensing: A survey. *ACM Computing Surveys (CSUR)* 54, 2 (2021), 1–35.

[45] LI, H., LUO, Y., GU, T., AND CHANG, L. Bffn: A novel balanced feature fusion network for fair facial expression recognition. *Engineering Applications of Artificial Intelligence* 138 (2024), 109277.

[46] LI, J., CHEN, T., AND TENG, S. A comprehensive survey on client selection strategies in federated learning. *Computer Networks* (2024), 110663.

[47] LI, M., GJORESKI, M., BARBIERO, P., SLAPNIČAR, G., LUŠTREK, M., LANE, N. D., AND LANGHEINRICH, M. A survey on federated learning in human sensing. *arXiv preprint arXiv:2501.04000* (2025).

[48] LI, Y., WANG, X., AND AN, L. Hierarchical clustering-based personalized federated learning for robust and fair human activity recognition. *Proceedings of the ACM on Interactive, Mobile, Wearable and Ubiquitous Technologies* 7, 1 (2023), 1–38.

[49] LIM, W. Y. B., LUONG, N. C., HOANG, D. T., JIAO, Y., LIANG, Y.-C., YANG, Q., NIYATO, D., AND MIAO, C. Federated learning in mobile edge networks: A comprehensive survey. *IEEE Communications Surveys & Tutorials* 22, 3 (2020), 2031–2063.

[50] LIU, Q., SUN, S., LIANG, Y., XUE, J., AND LIU, M. Personalized federated learning for spatio-temporal forecasting: A dual semantic alignment-based contrastive approach. *arXiv preprint arXiv:2404.03702* (2024).

[51] LU, X., ZHANG, Y., ZOU, H., LIANG, Y., WANG, W., AND CROWCROFT, J. Fedcom: Efficient personalized federated learning by finding your best peers. In *Proceedings of the 2nd ACM Workshop on Data Privacy and Federated Learning Technologies for Mobile Edge Network* (2023), pp. 107–112.

[52] LYMBEROPoulos, D., BAMIS, A., AND SAVVIDES, A. A methodology for extracting temporal properties from sensor network data streams. In *Proceedings of the 7th international conference on Mobile systems, applications, and services* (2009), pp. 193–206.

[53] MASHHADI, A., TABARAEI, A., ZHAN, Y., AND PARIZI, R. M. An auditing framework for analyzing fairness of spatial-temporal federated learning applications. In *2022 IEEE World AIoT Congress (AIoT)* (2022), IEEE, pp. 699–707.

[54] McCARTHY, C., PRADHAN, N., REDPATH, C., AND ADLER, A. Validation of the empatica e4 wristband. In *2016 IEEE EMBS international student conference (ISC)* (2016), IEEE, pp. 1–4.

[55] McMAHAN, B., MOORE, E., RAMAGE, D., HAMPSON, S., AND Y ARCAS, B. A. Communication-efficient learning of deep networks from decentralized data. In *Artificial intelligence and statistics* (2017), PMLR, pp. 1273–1282.

[56] MEHRABI, N., MORSTATTER, F., SAXENA, N., LERMAN, K., AND GALSTYAN, A. A survey on bias and fairness in machine learning. *ACM computing surveys (CSUR)* 54, 6 (2021), 1–35.

[57] MOHRI, M., SIVEK, G., AND SURESH, A. T. Agnostic federated learning. In *International Conference on Machine Learning* (2019), PMLR, pp. 4615–4625.

[58] NAGPAL, R., SHAHSARIFAR, R., GOYAL, V., AND GUPTA, A. Optimizing fairness and accuracy: a pareto optimal approach for decision-making. *AI and Ethics* 5, 2 (2025), 1743–1756.

[59] PADH, K., ANTOGNINI, D., LEJAL-GLAUME, E., FALTINGS, B., AND MUSAT, C. Addressing fairness in classification with a model-agnostic multi-objective algorithm. In *Uncertainty in artificial intelligence* (2021), PMLR, pp. 600–609.

[60] PAPADAKI, A., MARTINEZ, N., BERTRAN, M., SAPIRO, G., AND RODRIGUES, M. Minimax demographic group fairness in federated learning. In *Proceedings of the 2022 ACM Conference on Fairness, Accountability, and Transparency* (2022), pp. 142–159.

[61] PAPADAKI, A., MARTINEZ, N., BERTRAN, M., SAPIRO, G., AND RODRIGUES, M. Federated fairness without access to sensitive groups. *arXiv preprint arXiv:2402.14929* (2024).

[62] PESSACH, D., AND SHMUEL, E. A review on fairness in machine learning. *ACM Computing Surveys (CSUR)* 55, 3 (2022), 1–44.

[63] PIRTTIKANGAS, S., FUJINAMI, K., AND NAKAJIMA, T. Feature selection and activity recognition from wearable sensors. In *Ubiquitous Computing Systems: Third International Symposium, UCS 2006, Seoul, Korea, October 11–13, 2006. Proceedings* 3 (2006), Springer, pp. 516–527.

[64] PUCCINELLI, D., AND HAENGGI, M. Wireless sensor networks: applications and challenges of ubiquitous sensing. *IEEE Circuits and systems magazine* 5, 3 (2005), 19–31.

[65] RIEKE, N., HANCOX, J., LI, W., MILLETARI, F., ROTH, H. R., ALBARQOUNI, S., BAKAS, S., GALTIER, M. N., LANDMAN, B. A., MAIER-HEIN, K., ET AL. The future of digital health with federated learning. *NPJ digital medicine* 3, 1 (2020), 1–7.

[66] SATHYA, D., CHAITHRA, V., ADIGA, S., SRUJANA, G., AND PRIYANKA, M. Systematic review on on-air hand doodle system for the purpose of authentication. In *2023 Third International Conference on Artificial Intelligence and Smart Energy (ICAIS)* (2023), IEEE, pp. 1460–1467.

[67] SHAHBAZIAN, R., AND TRUBITSYNA, I. Human sensing by using radio frequency signals: A survey on occupancy and activity detection. *IEEE Access* (2023).

[68] SHAIK, T., TAO, X., HIGGINS, N., GURURAJAN, R., LI, Y., ZHOU, X., AND ACHARYA, U. R. Fedstack: Personalized activity monitoring using stacked federated learning. *Knowledge-Based Systems* 257 (2022), 109929.

[69] SHARMA, H., XIAO, Y., TUMANOVA, V., AND SALEKIN, A. Psychophysiological arousal in young children who stutter: An interpretable ai approach. *Proceedings of the ACM on interactive, mobile, wearable and ubiquitous technologies* 6, 3 (2022), 1–32.

[70] SINGH, S. P., AND ALISTARH, D. Woodfisher: Efficient second-order approximation for neural network compression. *Advances in Neural Information Processing Systems* 33 (2020), 18098–18109.

[71] THOMAS, V., PEDREGOSA, F., MERRIENBOER, B., MANZAGOL, P.-A., BENGIO, Y., AND ROUX, N. L. On the interplay between noise and curvature and its effect on optimization and generalization. In *Proceedings of the Twenty Third International Conference on Artificial Intelligence and Statistics* (June 2020), PMLR, pp. 3503–3513. ISSN: 2640-3498.

[72] TRAN, C. *The Interplay Between Privacy and Fairness in Learning and Decision Making Problems*. PhD thesis, Syracuse University, 2023.

[73] TRAN, C., FIORETTI, F., KIM, J.-E., AND NAIDU, R. Pruning has a disparate impact on model accuracy. *Advances in Neural Information Processing Systems* 35 (2022), 17652–17664.

[74] VOS, G., TRINH, K., SARNYAI, Z., AND AZGHADI, M. R. Generalizable machine learning for stress monitoring from wearable devices: A systematic literature review. *International Journal of Medical Informatics* (2023), 105026.

[75] WANG, D., SZYMANSKI, B. K., ABDELAZHER, T., JI, H., AND KAPLAN, L. The age of social sensing. *Computer* 52, 1 (2019), 36–45.

[76] WANG, F., HAN, J., ZHANG, S., HE, X., AND HUANG, D. Csi-net: Unified human body characterization and pose recognition. *arXiv preprint arXiv:1810.03064* (2018).

[77] WANG, T., WANG, Z., AND YU, J. Zeroth-order low-rank hessian estimation via matrix recovery. *arXiv preprint arXiv:2402.05385* (2024).

[78] WU, C., WANG, H., ZHANG, X., FANG, Z., AND BU, J. Spatio-temporal heterogeneous federated learning for time series classification with multi-view orthogonal training. In *Proceedings of the 32nd ACM International Conference on Multimedia* (2024), pp. 2613–2622.

[79] XIAO, Y., SHARMA, H., ZHANG, Z., BERGEN-CICO, D., RAHMAN, T., AND SALEKIN, A. Reading between the heat: Co-teaching body thermal signatures for non-intrusive stress detection. *Proceedings of the ACM on Interactive, Mobile, Wearable and Ubiquitous Technologies* 7, 4 (2024), 1–30.

[80] XU, X., LIU, X., ZHANG, H., WANG, W., NEPAL, S., SEFIDGAR, Y., SEO, W., KUEHN, K. S., HUCKINS, J. F., MORRIS, M. E., ET AL. Globem: Cross-dataset generalization of longitudinal human behavior modeling. *Proceedings of the ACM on Interactive, Mobile, Wearable and Ubiquitous Technologies* 6, 4 (2023), 1–34.

[81] Xu, Z., ZHAO, S., QUAN, Q., YAO, Q., AND ZHOU, S. K. Fairadabn: Mitigating unfairness with adaptive batch normalization and its application to dermatological disease classification. In *International Conference on Medical Image Computing and Computer-Assisted Intervention* (2023), Springer, pp. 307–317.

[82] YANG, J., CHEN, X., WANG, D., ZOU, H., LU, C. X., SUN, S., AND XIE, L. Sensefi: A library and benchmark on deep-learning-empowered wifi human sensing. *Patterns* 4, 3 (2023).

[83] YAO, D., ZHU, Z., LIU, T., XU, Z., AND JIN, H. Rethinking personalized federated learning from knowledge perspective. In *Proceedings of the 53rd International Conference on Parallel Processing* (2024), pp. 991–1000.

[84] YFANTIDOU, S., CONSTANTINIDES, M., SPATHIS, D., VAKALI, A., QUERCIA, D., AND KAWSAR, F. Beyond accuracy: A critical review of fairness in machine learning for mobile and wearable computing. *arXiv preprint arXiv:2303.15585* (2023).

[85] YFANTIDOU, S., CONSTANTINIDES, M., SPATHIS, D., VAKALI, A., QUERCIA, D., AND KAWSAR, F. The state of algorithmic fairness in mobile human-computer interaction. In *Proceedings of the 25th International Conference on Mobile Human-Computer Interaction* (2023), pp. 1–7.

[86] YFANTIDOU, S., SERMPEZIS, P., VAKALI, A., AND BAEZA-YATES, R. Uncovering bias in personal informatics. *Proceedings of the ACM on*

Interactive, Mobile, Wearable and Ubiquitous Technologies 7, 3 (2023), 1–30.

[87] ZANNA, K., AND SANO, A. Enhancing fairness and performance in machine learning models: A multi-task learning approach with monte-carlo dropout and pareto optimality. *arXiv preprint arXiv:2404.08230* (2024).

[88] ZENG, Y., CHEN, H., AND LEE, K. Improving fairness via federated learning. *arXiv preprint arXiv:2110.15545* (2021).

[89] ZHANG, D. Y., KOU, Z., AND WANG, D. Fairfl: A fair federated learning approach to reducing demographic bias in privacy-sensitive classification models. In *2020 IEEE International Conference on Big Data (Big Data)* (2020), IEEE, pp. 1051–1060.

[90] ZHANG, H., WANG, L., SHENG, Y., XU, X., MANKOFF, J., AND DEY, A. K. A framework for designing fair ubiquitous computing systems. In *Adjunct Proceedings of the 2023 ACM International Joint Conference on Pervasive and Ubiquitous Computing & the 2023 ACM International Symposium on Wearable Computing* (2023), pp. 366–373.

[91] ZHANG, H., YUAN, X., AND PAN, S. Unraveling privacy risks of individual fairness in graph neural networks. In *2024 IEEE 40th International Conference on Data Engineering (ICDE)* (2024), IEEE, pp. 1712–1725.

[92] ZHANG, T., GAO, L., LEE, S., ZHANG, M., AND AVESTIMEHR, S. Timelyfl: Heterogeneity-aware asynchronous federated learning with adaptive partial training. In *Proceedings of the IEEE/CVF Conference on Computer Vision and Pattern Recognition* (2023), pp. 5064–5073.

[93] ZHANG, W., AND NTOUTSI, E. Faht: an adaptive fairness-aware decision tree classifier. *arXiv preprint arXiv:1907.07237* (2019).

[94] ZHANG, Y., ZHENG, Y., QIAN, K., ZHANG, G., LIU, Y., WU, C., AND YANG, Z. Widar3. 0: Zero-effort cross-domain gesture recognition with wi-fi. *IEEE Transactions on Pattern Analysis and Machine Intelligence* 44, 11 (2021), 8671–8688.

[95] ZHAO, Y., LI, M., LAI, L., SUDA, N., CIVIN, D., AND CHANDRA, V. Federated learning with non-iid data. *arXiv preprint arXiv:1806.00582* (2018).

[96] ZHOU, Z., CHEN, X., LI, E., ZENG, L., LUO, K., AND ZHANG, J. Edge intelligence: Paving the last mile of artificial intelligence with edge computing. *Proceedings of the IEEE* 107, 8 (2019), 1738–1762.

[97] ZHU, L., LIN, H., LU, Y., LIN, Y., AND HAN, S. Delayed gradient averaging: Tolerate the communication latency for federated learning. *Advances in neural information processing systems* 34 (2021), 29995–30007.

A Methodological Transparency & Reproducibility Appendix (META)

A.1 Dataset and Model Description

This section provides a detailed overview of the dataset and the models we utilized in our evaluations.

A.1.1 Dataset Description. WIDAR Dataset: The WIDAR3.0 dataset [94] contains WIFI channel state information (CSI) [36] which represents the variation in the Wifi channel portrayed by commodity wifi devices [36, 94]. The WIFI CSI contains fine-grained information about variations in the Wifi channel based on the Doppler phenomenon [94]. These signals have been used by prior researchers for gesture detection [94], presence detection [66], pose estimation [76], human identification and activity detection [67]. We have used it as one of the HAR (Human Activity Recognition) datasets. The dataset contains data from 16 participants, 4 Females, and 12 Males, with five different orientations (labeled as 1 to 5). We removed a female participant from the dataset due to the absence of ground truth. The selected two gestures, ‘Slide’ and ‘Sweep,’ had data in all orientations for male and female participants in the presence of the wifi sensor. Since all participants had an equal number of samples in different orientations, i.e., orientations 1 to 5, we created a disparity in the dataset based on orientations by randomly sub-sampling 50% of the data belonging to orientations 4 and 5. This was done to create a training imbalance representative of real-life scenarios where some groups have more representation compared to others. We considered labels 1 to 3 as major orientation and the rest as minor orientation. For our work, we have trained a model to perform binary classification to detect Sweep vs. Slide gestures using WIFI-CSI data and fairness on the basis of ‘sex’ and ‘orientation’ as sensitive attributes.

HuGaDB Dataset: We have also utilized the HuGaDB (Human Gait Database) dataset [12] for HAR purposes, which comprises a diverse array of human activity recordings from 18 participants. The participant group includes 4 females and 14 males. In our work, we trained a binary classification model to distinguish between Standing and other activities from this dataset, with fairness considerations based on ‘sex’ as the sensitive attribute.

Stress sensing Dataset: Xiao et al. [79] collected this dataset. This dataset was obtained from 48 individuals, including 40 females and 8 males, who participated in four different stress-inducing tasks (Arithmetic, Bad Memory, Stress Videos, Pre-condition), each associated with unique stressors. The dataset is not publicly available yet; Access to the dataset has been obtained through proper IRB approvals/extensions. Due to the continuation of data collection by the Xiao et al. [79]’s research group, this paper’s reported dataset has more individuals than reported by the Xiao et al. [79] paper. The dataset has individuals wearing Empatica E4 [54] (collecting Stresssensing data) in their left and/or right hands and individuals’ sex information. Hence, this paper utilized ‘hand’ information and ‘sex’ as sensitive attributes for evaluation. Utilizing this dataset, we performed a binary stress detection classification task.

A.1.2 Client Distribution: Distinct client distributions are established for each dataset in our study.

- To effectively benchmark the performance of our proposed model and ensure clients with diverse participant groups, we deliberately structured the client distribution to include at least one participant from each sensitive attribute category. Table 10 provides a detailed overview of participant distribution across clients, categorizing them based on the sensitive attributes of males and females.
- Given that our models do not depend on sensitive attribute information during training, we also demonstrate their effectiveness by emulating the approach in clients with either single and/or multiple participants. This intentional diversification, as depicted in Table 11, does not guarantee the presence of both sensitive attributes within each client.

A.1.3 Model Description. WIDAR Model: The WIDAR Model architecture (adapted from [82]) is comprised of two fully connected layers within a sequential module, featuring an input size of $22 * 20 * 20$. A dropout layer with a 40% dropout rate and a Rectified Linear Unit (ReLU) activation function follow the first linear layer, while

Dataset	Clients	Male	Female
WIDAR	Client 1	4	1
	Client 2	4	1
	Client 3	4	1
HugaDB	Client 1	4	1
	Client 2	4	1
	Client 3	4	1
	Client 4	2	1
Stress sensing	Client 1	2	4
	Client 2	4	2
	Client 3	1	6
	Client 4	1	6
	Client 5	2	3
	Client 6	1	7
	Client 7	3	6

Table 10. Random distribution of multi-person clients of WIDAR, HugaDB, and Stress sensing Datasets.

Dataset	Clients	Male	Female
WIDAR	Client 1	1	1
	Client 2	2	1
	Client 3	1	0
	Client 4	2	0
	Client 5	2	1
	Client 6	1	0
	Client 7	1	0
	Client 8	2	0
HugaDB	Client 1	6	0
	Client 2	5	1
	Client 3	0	2
	Client 4	0	1
Stress sensing	Client 1	1	0
	Client 2	3	0
	Client 3	6	10
	Client 4	0	6
	Client 5	3	7
	Client 6	2	9
	Client 7	0	1

Table 11. Single and multi-person clients distribution across WIDAR, HugaDB and Stress sensing Datasets

the second linear layer outputs the classification result. The model reshapes the input tensor during the forward pass and incorporates dropout layers to mitigate over-fitting.

HugaDB Model: The HugaDB model architecture (adapted from [63]) is characterized by its complexity, featuring two sequential fully connected layers. The first layer consists of linear transformations with input and

output sizes of 792 to 1024, followed by dropout with a 30% probability, Rectified Linear Unit (ReLU) activation, and Instance Normalization. Subsequently, another linear layer reduces the dimensionality to 512, followed by similar dropout, ReLU, and Instance Normalization. The second layer further reduces the dimensionality from 512 to 128, followed by a linear layer with an output size equal to the specified number of classes. The final output is obtained by applying the sigmoid function to the result. During the forward pass, the input tensor is processed through these layers, reshaped when necessary, and the output is returned after applying the sigmoid function.

Stress sensing Model: The Stress sensing model architecture (adapted from [69]) comprises three sequential fully connected layers. The first layer takes input of size 34 and produces an output of size 64, incorporating batch normalization and Rectified Linear Unit (ReLU) activation. The second layer further processes the output, reducing it to size 128 with ReLU activation. The final layer transforms the output to the specified embedding size.

A.1.4 Hyperparameters. We have produced results from three different seed sets and presented one of them here. The complete set of results for all three seeds can be found in Table 12.

Dataset	F1 Score	Accuracy	EO Gap	Model	Seed
HugaDB	0.8568	0.8501	0.4192	fedavg	123
	0.8702	0.8654	0.3988	CurvFed	123
	0.8496	0.8425	0.4369	fedavg	16
	0.8856	0.8819	0.3952	CurvFed	16
	0.8548	0.8476	0.4318	fedavg	12345
	0.8896	0.8859	0.4012	CurvFed	12345
Stress sensing	0.7466	0.7473	0.3316	fedavg	123
	0.7901	0.7868	0.2469	CurvFed	123
	0.7383	0.7385	0.3086	fedavg	12345
	0.7944	0.7912	0.2557	CurvFed	12345
	0.7235	0.7253	0.3069	fedavg	2023
	0.7814	0.7780	0.2522	CurvFed	2023
WIDAR	0.8645	0.8643	0.4199	fedavg	123
	0.7818	0.7906	0.2983	CurvFed	123
	0.8645	0.8643	0.4136	fedavg	12345
	0.7897	0.7960	0.3086	CurvFed	12345
	0.8507	0.8602	0.4264	fedavg	2023
	0.8100	0.8123	0.3534	CurvFed	2023

Table 12. Performance metrics (F1, Accuracy, EO Gap) for FL models with different seeds across datasets

The approach uses several hyperparameters for Benign and **CurvFed** model training. Table 13 and 14 shows the hyperparameter values for benign and **CurvFed** model training, respectively. These values correspond to the best results obtained using a grid search. Within the context of the **CurvFed** model, the SWA Learning Rate specifically denotes the learning rate at which the SWA model is introduced into the training process. The SWA Start Round is indicative of the round at which the SWA mechanism is initiated. Additionally, the cycle parameter signifies that post the initiation of SWA, the global model and learning rate undergo updates using SWA in a cyclic manner, with each cycle representing a distinct iteration of this process. The term ϵ pertains to

the weighting value, which ensures the maintenance of the relative ranks of each client during the aggregation process. Opting for a smaller value of ϵ proved beneficial for better ranking precision.

Hyperparameter	WIDAR	Stress sensing	HugaDB
Learning Rate	0.1	0.1	0.001
Epochs	3	3	3
Total Round	80	80	100

Table 13. Hyperparameters for benign Fedavg model

B Experiment Details

B.1 Details of ablation study

We conducted a comprehensive ablation study to meticulously guide the choices in our proposed approach. The study consistently demonstrates the effectiveness of our model across all datasets.

B.1.1 The Independent Effect of Sharpness-aware Aggregation and its Ablation Analysis. This section evaluates the effect of Sharpness-aware aggregation on enhancing FWD independently.

Previous studies have explored benign client-side training, using various weighted aggregation schemes to promote fairness [23]. **CurvFed**, for instance, aligns with Pessimistic Weighted Aggregation (P-W), a method that excludes highly biased (based on known bias-creating factors) models during aggregation. However, **CurvFed** takes a different approach, assigning lower weights to highly biased (based on loss-landscape sharpness; without the knowledge of the bias-creating factors) and low-efficacy local client-side models, thereby promoting fairness without completely excluding them.

To understand the benefits of **CurvFed**'s Sharpness-aware aggregation strategy independently (without client-side local training fairness constraints) in promoting clients with both (1) low error rates and (2) lower maximal uncertainty we evaluated three following variations, while all of them maintaining benign local client-side training without any fairness objectives.

- **CurvFed**'s aggregation strategy as outlined in Equation 12 of the main paper while maintaining benign local client-side training without any fairness objectives.
- **CurvFed**'s aggregation strategy modification, where just selecting clients with lower maximal uncertainty in prediction (Based on T in Equation 12), while maintaining benign local client-side training without any fairness objectives.

Hyperparameter	WIDAR	Stress sensing	HugaDB
Learning Rate	0.01	0.01	0.001
SWA Learning Rate	0.1	0.001	0.001
SWA start round	16	16	16
cycle	5	5	3
Epochs	3	3	3
alpha	0.92	0.92	0.92
ϵ	0.005	0.005	0.005
Total Rounds	80	80	80

Table 14. Hyperparameters for proposed **CurvFed** model

Dataset	Client-Side Training	Aggregation Strategy	F1 Score	EO Gap	FATE Score $\times 10^{-1}$
WIDAR	Benign	Fedavg	0.8507	0.4263	0
	SAM	Fedavg	0.8005	0.4251	-0.560
	SAM	Fedswa	0.8405	0.4071	0.331
	SAM+ $\lambda(F_{client})$ (Eq11)	Fedswa	0.8459	0.4058	0.424
	$\lambda(F_{client})$ (Eq11)	Fedavg	0.8253	0.3994	0.332
	$\lambda(F_{client})$ (Eq11)	W^r (Eq12)	0.8344	0.4135	0.109
	SAM+ $\lambda(F_{client})$ (Eq11)	W^r (Eq12)	0.8707	0.4199	0.386
Stress sensing	$\lambda(F_{client})$ (Eq11)	Sharpness Aware aggregation	0.8409	0.3982	0.545
	SAM	Fedswa+S(L) (Eq12)	0.8737	0.4199	0.420
	SAM	Fedswa+S(T) (Eq12)	0.8590	0.4084	0.518
	SAM	Sharpness Aware aggregation	0.8668	0.4161	0.429
	SAM+ $\lambda(F_{client})$ (Eq11)	Sharpness Aware aggregation	0.8100	0.3533	1.233
	Benign	Fedavg	0.7253	0.3069	0
	SAM	Fedavg	0.7758	0.3034	0.812
HugaDB	SAM	Fedswa	0.7406	0.3015	0.384
	SAM+ $\lambda(F_{client})$ (Eq11)	Fedswa	0.7346	0.2768	1.105
	$\lambda(F_{client})$ (Eq11)	Fedavg	0.7372	0.2998	0.395
	$\lambda(F_{client})$ (Eq11)	W^r (Eq12)	0.7345	0.2839	0.874
	SAM+ $\lambda(F_{client})$ (Eq11)	W^r (Eq12)	0.8193	0.2927	1.756
	$\lambda(F_{client})$ (Eq11)	Sharpness Aware aggregation	0.7077	0.2380	1.999
	SAM	Fedswa+S(L) (Eq12)	0.8091	0.2680	2.240
	SAM	Fedswa+S(T) (Eq12)	0.7995	0.2627	2.46
	SAM	Sharpness Aware aggregation	0.8224	0.2710	2.507
	SAM+ $\lambda(F_{client})$ (Eq11)	Sharpness Aware aggregation	0.7814	0.2522	2.555
	Benign	Fedavg	0.8496	0.4369	0
	SAM	Fedavg	0.8555	0.4255	0.329
	SAM	Fedswa	0.8418	0.4242	0.192
	SAM+ $\lambda(F_{client})$ (Eq11)	Fedswa	0.8170	0.4142	0.135
	$\lambda(F_{client})$ (Eq11)	Fedavg	0.8567	0.4142	0.602
	$\lambda(F_{client})$ (Eq11)	W^r (Eq12)	0.8574	0.4083	0.746
	SAM+ $\lambda(F_{client})$ (Eq11)	W^r (Eq12)	0.9016	0.4154	1.103
	$\lambda(F_{client})$ (Eq11)	Sharpness Aware aggregation	0.8510	0.4333	0.0982
	SAM	Fedswa+S(L) (Eq12)	0.8934	0.4130	1.059
	SAM	Fedswa+S(T) (Eq12)	0.8888	0.4142	0.878
	SAM	Sharpness Aware aggregation	0.8911	0.4095	1.11
	SAM+ $\lambda(F_{client})$ (Eq11)	Sharpness Aware aggregation	0.8855	0.3952	1.376

Table 15. Performance metrics on the different datasets for different FL strategies and model configurations

- **CurvFed**'s aggregation strategy modification, where just selecting clients with lower error rate (Based on L in Equation 3), while maintaining benign local client-side training without any fairness objectives.

The evaluation results are presented in rows highlighted in ‘blue’ in Table 15. First, these results consistently demonstrate that across all datasets, **CurvFed**'s aggregation strategy, as outlined in Equations 2 and 3, outperforms

others. Meaning this evaluation confirms that integrating both classification and top eigenvalue loss and favoring clients with lower loss (as outlined in Equations 2 and 3) enhances the balance between efficacy and fairness.

Furthermore, the fact that fairer models are achieved even without local client-side fairness constraints in these evaluations, compared to the benign baselines presented in rows highlighted in ‘red’ in Table 15, establishes that **CurvFed**’s Sharpness-aware aggregation independently promotes FWD.

B.1.2 The Independent Effect of Sharpness-aware Client-side Local Training. This section evaluates the independent effect of Sharpness-aware client-side local training as outlined in Equation 1 to enhance FWD. To conduct this evaluation, we implemented a variant where client-side local training incorporates fairness constraints based on Equation 1, while employing a benign aggregation scheme where all weights in Equation 2 are set to ‘1.’ To ensure a fair comparison, the SWA aggregation strategy, outlined in Algorithm 1, remains employed in this approach. The evaluation results are showcased in rows highlighted in ‘yellow’ in Table 15, indicating its superior enhancement of fairness compared to the benign approaches depicted in ‘red’ highlighted rows across all datasets. This underscores the independent influence of client-side sharpness-aware local training in enhancing FWD.

B.1.3 Independent Effect of FIM penalty term in Client-side training and Aggregation. In this section, we explore the independent effect of FIM penalty in the client-side training process and its interaction with various aggregation strategies. In our experiments, marked in orange, we observed that incorporating top eigenvalue of FIM either in the client-side training or aggregation, or having both without sharpness-aware strategies like SAM and SWA, leads to a fairer model, as indicated by a reduced EO Gap. However, this improvement in fairness comes at the cost of model accuracy, which tends to decrease.

The next observation shows that SAM significantly boosts the accuracy of the model, but this improvement comes at the cost of fairness, as reflected by a greater EO Gap. This suggests that SAM enhances model performance in terms of accuracy but introduces a trade-off in fairness.

For example, in the WIDAR dataset, applying the penalty term FIM penalty in client-side training while keeping the aggregation strategy benign reduces the EO Gap from 0.4263 (Benign) to 0.4186, reflecting a fairness improvement. However, this comes with a decline in F1 score, dropping from 0.8507 to 0.8394. Replacing the benign aggregation with a weighted strategy (W') further improves fairness, reducing the EO Gap to 0.4135, though the F1 score slightly decreases again to 0.8359. In contrast, using SAM in client-side training increases the F1 score to 0.8587, indicating enhanced model performance. Yet, this setting shows limited improvement in fairness, with the EO Gap remaining relatively high at 0.4212. This demonstrates that while SAM is effective for boosting accuracy, it does little to mitigate fairness issues. Interestingly, a more balanced configuration emerges when FIM penalty is applied without SAM in training and paired with sharpness aware aggregation. This setup achieves an F1 score of 0.8574 while also keeping the EO Gap at 0.4148, offering a better trade-off between fairness and accuracy. In the Stress Sensing dataset, applying the regularization term FIM penalty in client-side training while using FedAvg aggregation leads to a significant reduction in EO Gap, from 0.3069 (Benign) to 0.2539, indicating improved fairness. However, this results in a drop in F1 score from 0.7253 to 0.7034, reflecting a loss in model performance. On the other hand, SAM increases the F1 score to 0.7758, the highest among all settings, but only slightly improves fairness (EO Gap = 0.3034), showing again that SAM prioritizes accuracy over fairness. In the HugaDB dataset, applying FIM penalty with FedAvg yields the lowest EO Gap of 0.3928, improving fairness by over 10% compared to the baseline (0.4369), and even increases the F1 score to 0.8634, surpassing the benign setup. However, using SAM alone pushes the F1 score higher to 0.8789, but fairness drops slightly with EO Gap rising to 0.4000.

These findings emphasize the importance of incorporating our top eigenvalue of FIM regularization term in local training and aggregation strategies in server with sharpness-aware techniques like SAM or SWA. By doing so, we can strike a better balance between fairness and accuracy, ensuring the model performs well on both metrics.

B.1.4 Importance of Integrating Sharpness-Aware Client-side Training and Aggregation Strategy for FWD. The evaluations discussed above have demonstrated that both the Sharpness-Aware Aggregation Strategy, outlined in Equations 2 and 3, and the Sharpness-Aware client-side local training, depicted by Equation 1 in the main paper, independently contribute to promoting fairness. However, these individual strategies exhibit less effectiveness (fairness and efficacy balance) compared to the presented **CurvFed** approach, which incorporates both strategies, as indicated by the ‘green’ highlighted rows across all datasets in Table 15. This underscores the effectiveness of Algorithm 1 in attaining FWD.